UPTEC W 23009
Examensarbete 30 hp
Juni 2023

UPPSALA
UNIVERSITET

The influence of infiltration capacity and antecedent soil moisture conditions on urban pluvial flooding

Disa Barkefors

Civilingenjörsprogrammet i miljö- och vattenteknik

UPPSALA UNIVERSITET

The influence of infiltration capacity and antecedent soil moisture conditions on urban pluvial flooding

Disa Barkefors

Abstract

Urban pluvial floods occur during extreme rain events and both occurrence and magnitude of these floods are expected to increase. Preserving or constructing green areas in urban areas has been shown to mitigate and control these floods. The common way to evaluate flood risks is to set up a rainfall-runoff model, but these studies are often case related and only investigate the soil characteristics for that specific case. Multiple studies have also stated that the difference between major and minor flooding effects is connected to the antecedent soil moisture content. This thesis attempts to investigate how different soil characteristics influencing infiltration affect the hydraulic response in two Swedish urban catchments and if antecedent soil moisture is a critical factor.

To evaluate the hydraulic response, a two-dimensional surface runoff model of two different urban catchments was forced with a hyetograph of a CDS-rain with a return period of 100 years. The simulations were conducted with three different soil types for all urban green areas: clay, sandy loam and sand, and three different antecedent soil moisture contents for clay and sandy loam. Flood extent and discharge from catchment area was evaluated, as was flood depth and overland flow in 16 chosen evaluation points.

The results showed that with decreasing infiltration rate of a soil and with increasing antecedent soil moisture content, the severity of the flood and discharge at the catchment outlet was increased. It was also concluded that soil type affects flood extent, flood depth, overland flow and discharge from catchment to a greater extent than antecedent soil moisture.

Key words: Urban pluvial flood, 2D modelling, MIKE+, urban green area, soil moisture, Chicago Design Storm

Teknisk-naturvetenskapliga fakulteten

Uppsala universitet, Utgivningsort Uppsala

Handledare: Johan Kjellin Ämnesgranskare: Benjamin Fischer

Examinator: Fritjof Fagerlund

Referat

Infiltration och tidigare markförhållandens inverkan på urbana översvämningar

Disa Barkefors

Pluviala översvämningar i urbana grönområden inträffar under extrema regnhändelser och både förekomsten och omfattningen av dessa översvämningar förväntas öka. Att bevara eller bygga urbana grönområden har visat sig mildra och kontrollera dessa översvämningar. Det vanligaste sättet att utvärdera översvämningsrisker är att konstruera en avrinningsmodell, men dessa studier är ofta fallrelaterade och undersöker bara markegenskaperna för det specifika fallet. Flera studier har också angett att det är vattenhalten i marken vid regnets start som styr hur allvarliga översvämningskonsekvenserna blir. Detta examensarbete undersöker hur olika markegenskaper som påverkar infiltrationen påverkar den hydrauliska responsen i ett avrinningsområde och om markens vattenhalt är en kritisk faktor.

För att utvärdera den hydrauliska responsen byggdes en tvådimensionell avrinningsmodell för två olika urbana avrinningsområden. Modellerna kördes med ett CDS-regn med en återkomstperiod på 100 år. Simuleringarna genomfördes med tre olika jordtyper för alla urbana grönområden: lera, sandig lerjord och sand, och tre olika vattenhalter för lera och sandig lerjord. Översvämningsutbredning och utflödet från avrinningsområdet utvärderades, liksom översvämningsdjup och ytavrinning i 16 utvalda utvärderingspunkter.

Resultaten visade att med minskande infiltrationshastighet i en jord och med ökande vattenhalt, ökade omfattningen av översvämningen samt utflödet från avrinningsområdet. En slutsats kunde också dras att jordarten påverkar översvämningsutbredning, översvämningsdjup, ytavrinning och utflöde från avrinningsområdet i större utsträckning än markens vattenhalt vid regnets start.

Nyckelord: Urbana översvämningar, 2D-modell, MIKE+, urbana grönområden, markvatten, Chicago Design Storm

Institutionen för Geovetenskaper, luft-, vatten- och landskapslära, Uppsala
Villavägen 16 SE-75236 Uppsala

ISSN 1401-15765

Preface

This master thesis finalizes the Master programme in Environmental and Water Engineering at Uppsala University and Swedish University of Agricultural Science. The thesis project was conducted in collaboration with Tyréns with Johan Kjellin as supervisor. The subject reader was Benjamin Fischer and examiner Fritjof Fagerlund, both at the Department of Earth Sciences at Uppsala University.

I would like to thank Johan Kjellin for making this thesis possible and Benjamin Fischer for the support throughout the process. A special thank you to Jimmy Olsson and Elin Andersson at Tyréns for helping with construction of models, to Sara Ekeroth and Julia Granlund for being my sounding board and to the rest of the colleagues at the Uppsala office for all encouragement during the making of this thesis.

Lastly, a huge thanks to friends and family who supported me, fed me and made this time even more memorable.

Disa Barkefors

Uppsala, June 2023

POPULÄRVETENSKAPLIG SAMMANFATTNING

Konsekvenserna av klimatförändringarna blir allt mer påtagliga världen över och den fortsatta ökningen av antropogena växthusgasutsläpp förväntas de bli mer och mer extrema. Med de ökande temperaturer klimatförändringarna medför accelererar även den hydrologiska cykeln. Detta orsakar inte enbart kraftigare skyfall utan även att skyfallen förekommer mer frekvent än tidigare. De områden som är särskilt känsliga för extremare klimat är våra städer. Vi har redan upplevt konsekvenserna efter skyfallet i Gävle 2021 där kostnaderna för att återställa staden uppgick till 335 miljoner kronor. Hur motståndskraftig en stad är mot översvämningar beror till viss del av andelen grönytor i området eftersom dessa dels kan infiltrera regn, dels sakta ned avrinningen. Med den ökande urbaniseringen behövs fler bostäder och annan infrastruktur och områden som tidigare varit grönytor byts ut mot hårdgjorda ytor. Att bevara eller ge plats åt nya grönområden i städer är därför av stor vikt i det förebyggande arbetet mot översvämningar. Men, det är inte bara grönområden i sig som är väsentligt, utan vilken jordtyp som används i grönområdet kan vara minst lika viktigt.

För att studera tidigare urbana översvämningar och för att förutspå framtida översvämningar kan skyfallskarteringar användas. Genom att simulera regnevent med olika intensitet och återkomsttid går det att utvärdera framtida risker och ta fram åtgärdsplaner i förebyggande syfte. Konsekvenserna vid extrema översvämningar är inte enbart en fråga om kostnad utan kan även vara en risk för människors hälsa och till och med liv. Under översvämningarna i Gävle rapporterade räddningspersonal om begränsad framkomlighet, något som kunde fått allvarliga konsekvenser vid nödsituationer. Att ta fram skyfallskarteringar är en resursfråga, både i tid och pengar. Därför utförs ofta förenklingar och generaliseringar av verkligheten. En viktig parameter som ofta ansätts som konstant är infiltrationen i grönområden, vilket inte överensstämmer med verkligheten då infiltrationen delvis beror av markens vattenhalt. Om det regnat kort innan ett extremregn finns risk att markmättnaden är hög vilket medför att betydligt mindre andel av regnet kommer infiltrera och modellen underskattar översvämningen. För att få en mer exakt bild av översvämningsriskerna bör därför markens vattenhalt vid regnets start inkluderas i modellen.

Denna studie syftar till att undersöka hur en förändring av jordtyp i urbana grönområden påverkar översvämningskonsekvenserna vid ett 100-års regn och huruvida markmättnaden vid regnets start är en kritisk faktor. Detta utfördes genom att konstruera en tvådimensionell avrinningsmodell över två modellområden med olika andel grönytor respektive icke-permeabla ytor för att sedan simulera ett CDS-regn baserat på svenska förhållanden. Grönytornas egenskaper varierades mellan simuleringarna och totalt undersöktes tre olika jordtyper: lera, sandig lerjord och sand. För de två förstnämnda användes även tre olika vattenhalter i jorden vid regnets start. För hela modellområdet undersöktes översvämnings-utbredning och ytavrinning ut ur avrinningsområdet och i 16 utvärderings-punkter undersöktes översvämningsdjup och ytavrinning.

Resultaten från studien påvisade att jordtypen har större inverkan på översvämnings-konsekvenserna än markmättnaden vid regnets start. För samtliga utvärderingsparametrar upptäcktes samma resultatmönster: med minskande infiltrationshastighet och ökande markmättnad blev översvämningskonsekvenserna större. Detta resultat var förväntat i och med att infiltrationen i jorden styr avrinningen. Samma mönster upptäcktes för markmättnad vid regnets start men skillnaderna i resultaten mellan de olika vattenhalterna var betydligt mindre. Att skillnaderna var så små var inte ett förväntat resultat baserat på tidigare studier. Vid anläggning av urbana grönområden är val av jordtyp av stor vikt om de ska uppfylla sitt syfte att mildra och kontrollera översvämningar i städer.

CONTENTS

1 INTRODUCTION

One major consequence of climate change is that global warming is shifting the hydrological cycle, causing it to accelerate. A warmer temperature globally intensifies the evaporation and thus a higher amount of water circulating in the atmosphere. This leads to more frequent and intense precipitation events, sometimes as unpredictable storms (Kuebler 2022). In the European Commission's Green Paper from 2007 Scandinavia was highlighted as one of the most vulnerable areas in Europe due to the predictions of increase in rainfall (Swedish Commission on Climate and Vulnerability 2007). Several public authorities in Sweden such as Naturvårdsverket and MSB reports an expected increase in precipitation and occurrence of intense cloudburst (MSB 2016; Naturvårdsverket 2023) Statistics from measured precipitation by SMHI indicates that there has already been an increase in annual average precipitation from 600 mm/year in 1970 to 700 mm/year in 2020 and it will continue to increase (SMHI 2022b). With increased precipitation there is also an increased risk of urban floods which primarily affect infrastructure as roads, buildings and collection systems (Naturvårdsverket 2023).

The magnitude of an urban pluvial flooding event depends on many different parameters: the intensity and duration of a rainfall event, land-use, soil properties of urban green areas and others (Fidal & Kjeldsen 2020). One preventative flood measure is to increase amount of green area, such as parks, which can mitigate urban stormwater runoff and control flooding due to infiltration. Therefore, the properties of the soil in these urban green spaces are important. A greater infiltration rate and infiltration capacity of the soil will generally lead to less surface runoff (Ren et al. 2020). But this only applies to a certain extent. During prolonged rainfall the soil can become close to saturated and remaining rain will be mostly direct runoff (Fidal & Kjeldsen 2020)

To evaluate risks of urban pluvial flooding and develop methods for flood risk management, several rainfall-runoff models have been developed during the last decade that also consider the need to adapt to climate change. But according to Cea & Costabile (2022) there is still no unified approach to modeling and managing urban flood issues in the context of climate change. There are multiple studies that investigate infiltration in urban green areas, however they are often based on current conditions in existing parks (Duan et al. 2011; Lan et al. 2019). A research gap has therefore been identified regarding investigating green areas impacts on urban floods if the soil type in these parks were to change or choice of soil type when constructing urban green areas.

Multiple studies have concluded that the difference between major and minor flooding effects can be explained by the antecedent soil moisture conditions. It is therefore of great importance to obtain accurate and timely data on antecedent soil moisture content (Ahlmer et al. 2018). Still, Fidal and Kjeldsen (2020) identified that antecedent soil moisture is a parameter that is often disregarded in many existing rainfall-runoff models. Instead, a fixed percentage for runoff or zero infiltration may be used for modelling in urban areas. This may lead to inaccurate predictions since high soil saturation might lead to direct runoff during a rainfall event with high intensity or if the soil is unsaturated some rain will be lost due to infiltration (Fidal & Kjeldsen 2020)

1.1 URBAN FLOODING

There are two main categories of urban flooding, fluvial or pluvial. Fluvial flooding occurs from rising water levels in lakes or watercourses, overtopping their banks, which floods adjacent urban area. The rising water levels are often caused by excessive rain or snowmelt (SMHI 2023b). Pluvial floodings are strictly rain related floods that occur during/after extreme rainfall which cannot infiltrate the ground or be evacuated by storm water drainage systems fast

enough. These events are predicted to increase in occurrence due to climate change which requires adaptations of urban areas (SMHI 2023b). Another cause for increase in occurrence is urbanisation. When urban areas are expanding and densified, the proportion of green spaces (with high infiltration) decreases to make room for new infrastructure and therefore increases the proportion of impervious surfaces and so also surface runoff (Ren et al. 2020).

Direct effects of urban pluvial flooding are severe injuries or even loss of life (at very extreme precipitation events), damage to infrastructure due to erosion and flooding and monetary clean-up costs. But there are also indirect effects, an often neglected consequence of flood events, which are of remobilization and redistribution of pollutants. Especially in industrial countries there is an increased pollutant discharge which may cause health risks, long-term socio-economic impacts, and environmental impact due to ecological effects (Crawford et al. 2022).

1.1.1 Previous events of urban pluvial flooding in Sweden

MSB has presented a statistical compilation of damage amount from flooding for municipalities in Sweden between year 2015 and 2019. Uppsala was the municipality with highest damage amount (around 90 million SEK) of which a majority of the damage claim could be linked to a singular cloudburst event in 2018 (MSB & SGI 2021). The cloudburst event in question was on 29th of July and weather station Uppsala Aut recorded 61 mm rain in two hours (SMHI 2023a). One major consequence was that Akademiska sjukhuset was flooded, fortunately there were no reports of serious complications (SVT Nyheter 2018) and the passage at the central station had a flood depth of one meter. According to Per Berg, a professor in landscape architecture at the Swedish University of Agricultural sciences, this flood could have been avoided it Uppsala had two large green areas close to the train tracks (Prammefors & Wass 2018).

In August 2021 Gävle area was exposed to a 1000-year storm event. Between 8 am on the 17th of August to 8am on the 18th an estimated 161,6 mm of rain fell over the city of Gävle. During the most intense two hours 101 mm rain fell, which was a new Swedish record (SMHI 2022a). There were no reported serious injuries, but they experienced short power cuts, difficulties for transportation of emergency service personnel, severe flooding, and damage to infrastructure (Gävle Kommun 2022). Multiple roads collapsed during the flood and the railway viaduct for Upplandsleden was reported to have a flood depth of 4.5 meters (Hallberg 2021). Estimated cost for Gävle municipality one year after the storm event was 335 million SEK (Gävle Kommun 2022).

1.2 URBAN GREEN AREAS

Urban green areas can be defined as “any vegetation found in the urban environment, including parks, open spaces, residential gardens or street trees” (Ren et al. 2020). Urban green areas fulfil a variety of purposes. They do not only improve the environment but also promotes human health and might mitigate effects of natural disasters. Trees and other vegetation can improve air quality by purifying air from pollutants, lower the temperature locally and promote biodiversity. If correctly designed and developed, urban green areas can also mitigate effects of natural disasters as floods, storms and fires (Grahn & Stoltz 2022). Impervious surfaces such as roads, parking lots and driveways and sidewalks dominate urban areas, and they can neither receive nor infiltrate stormwater to the same extent as surrounding landscape. Instead, excess stormwater is handled by drainage systems, ones which often are not dimensioned for the large amounts of water a heavy cloudburst or prolonged rain could entail (Boverket 2022). Boverket (2022) states that pervious urban surfaces such as parks and green areas are needed to manage, delay and to some extent infiltrate stormwater locally and can also purify stormwater. It would be too costly and complex to expand and re-dimension today's water and sewage systems for

the expected increase in precipitation due to climate change. To invest in urban green areas is therefore a cost-effective solution for flood prevention (Boverket 2022).

Besides climate regulation and mitigation of flooding, urban green areas have also been proven to have a positive impact on human health. Research show that there is a clear connection between good access to/live nearby nature area or parks and a reduced risk of both dying prematurely and getting cardiovascular diseases (Grahn & Stoltz 2022).

1.3 INFILTRATION

Flooding is closely linked to infiltration of water into the soil. Infiltration is simply expressed as the movement of water downwards through the soil surface. The water could either come from precipitation that directly hits the soil surface, irrigation or as water dripping of vegetation (Hendriks 2010). When the water flows within the soil the process is instead called percolation. Infiltration rate is used to describe the velocity at which waters enters (infiltrates) the soil, measured in water depth over elapsed time (mm/h). The infiltration capacity represents the maximum rate at which given soil can absorb water (Hendriks 2010).

There are many factors that influence infiltration rate of a soil. It is determined by the interaction of both chemical and physical soil characteristics which can vary due to multiple reasons such as location, compaction, and biological processes. Three of the main factors are texture, porosity, and moisture content of the soil (Haghnazari et al. 2015). An in-depth description on how these soil characteristics influence infiltration are presented Appendix A.

1.4 SURFACE RUNOFF

There are two main mechanisms that causes surface runoff. The first mechanism is called Horton overland flow (or infiltration excess overland flow) and it occurs if the intensity of a rainfall or snow melt exceed the grounds infiltration capacity (NE 2023). The water will instead start to flow horizontally across the surface. The second mechanism occurs when the ground, or soil, already is saturated, often when the ground water surface reaches ground level and no more water can infiltrate the ground. This is called saturation excess overland flow (NE 2023).

There are multiple factors affecting runoff, both meteorological and physical characteristics. Meteorological factors may be type of precipitation such as rain, snow or sleet or the intensity, amount, duration, and distribution of precipitation. It could also be high antecedent soil moisture conditions caused by previous precipitation event or direction of storm movement (USGS 2023). Physical characteristics affecting runoff are for example soil type, elevation and topography, vegetation, and drainage area. If there are any bodies of water such as lakes or ponds where water may be accumulated and prevent or delay runoff. Runoff concerning urbanised areas are highly affected by land use due to the large increase of impervious surfaces which disturbs natural surface-runoff patterns (USGS 2023).

1.5 SURFACE ROUGHNESS

The roughness of a surface highly influences the runoff and can be estimated with Manning's number (M). Hardened surfaces, such as roads and roofs, have low roughness and therefore low flow resistance which results in a higher runoff velocity. This gives a higher Manning's number. Permeable surfaces, like vegetated green areas, have a higher roughness which increases the flow resistance and lowers the runoff velocity. These surfaces are described with a low Manning's number (MSB 2017). Table 1 shows the recommended Manning's numbers for hardened and vegetated surfaces from MSB (MSB 2014).

Table 1. Manning's value (M) (MSB 2014)

Surface	Manning's number M ($m^{1/3}/s$)
Vegetated/green area	2
Hardened	50

The surface roughness does not only influence the runoff velocity but also flow paths and distribution of flood. When flooded, a surface with high roughness generates a more concave flooded surface. This is due to the flow resistance inhibiting the water from flowing quickly to the deepest part of a low point which results in a greater flood extent but lower water depths (MSB 2014).

1.6 DESIGN STORM AND CDS

A design storm represents a rainfall event (or other precipitation events) defined with amount of rainfall and distribution in space and time and are often used to determine a design peak discharge or design flood. The chosen storm event is often expressed in a specific return period, such as a 10-year or a 100-year storm event, meaning the probability of a storm of such magnitude occurring is in every 10 or 100 years respectively (Markolf et al. 2021). To construct a design storm, statistics from historical rain events is needed. Preferably from same area as chosen study area. From the statistics it is possible to derive an IDF curve (Intensity Duration Frequency curve) which describes the relationship between rainfall intensity and duration for a specific return period (Svenskt vatten 2011). For Swedish conditions, Dahlström's formula can be used to calculate an IDF-curve as seen below in Equation 1,

$$i_F = 190 \cdot F^{\frac{1}{3}} \cdot \frac{\ln(T_r)}{T_r^{0.98}} + 2 \quad (1)$$

where i_F is mean rainfall intensity (L/s, h), T_r represents rain duration (min) and F equals return period (years). The formula is revised from Swedish precipitation statistics and is accurate for duration periods up to 24 hours. To visualize a design storm a hyetograph can be used which is a graphical representation of the distribution of rainfall intensity over time (Svenskt vatten 2011).

One of the most used frequency-based methods to obtain a design storm is CDS (Chicago design storm), a method proposed by Keifer and Chu (1957). The original CDS used the IDF curve for Chicago, thereby the name Chicago design storm, but since it was developed it has been applied globally using adaptations for local conditions (Gong et al. 2016). A specific property of the CDS method is that it is derived from an IDF curve based on calculated maximum mean intensity for different rain durations. Figure 1 shows an example of a hyetograph of a unitless CDS rain. The r-value of a CDS rain represents the skewness factor at the peak which is the relationship between start time of rain to peak intensity and the total duration of the rain (Svenskt vatten 2011). Most commonly used r-value when constructing design storms derived from Swedish conditions is 0.37 (Berggren et al. 2014), which is also the recommended value by Svenskt Vatten (2011).

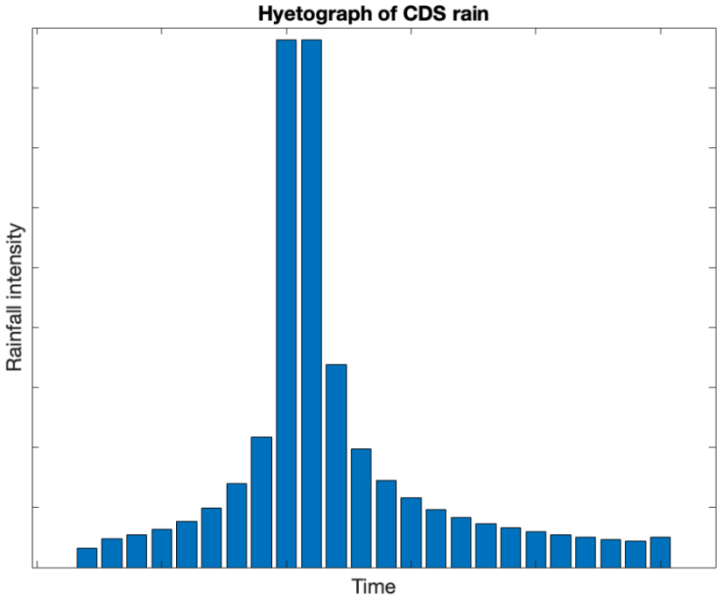

Figure 1. Unitless hyetograph of a CDS rain with time on the x-axis and rain intensity on the y-axis

When deciding on intensity and magnitude of a design storm for urban flood modelling with a simplified 2D surface runoff model (no drainage system), the load of the rain should with good margin exceed the capacity of the storm water management system. The uncertainty with a simplification disregarding a storm water management system increases as the difference between rain load and capacity of the system decreases. The recommendation from MSB is that a 2D surface runoff model should be conducted with a 100-year storm or more (MSB 2014).

1.7 2D SURFACE RUNOFF MODELLING

The simplest flooding analysis is identifying low points in the terrain, which are at risk of flooding during a rain event, by calculating maximum depth of the low points and the distribution. Generally, in this type of modelling all surfaces are assumed to be impermeable which entails no infiltration (MSB 2013). By adding properties of different surfaces in the studied area it is possible to conduct hydraulic calculations of surface runoff for real rain events, flow directions, flow speed and distribution of flooding (MSB 2014). This is called a two-dimensional surface runoff model. A 2D runoff model gives a generally good perception of large areas in relation to the computational time but does not account for the capacity of any collection system (storm water management system) in the studied area. This results in the dynamics of the flooding not being correctly captured where there is a collection system. If there is a collection system in the area, the best way is to connect the model to 1D hydraulic model for the collection system. This can be both time-consuming and difficult, especially if there is no information about the collection system. A simplified way to take the capacity into account is to deduct the expected rain load to be diverted by the collection system. Another method is to choose a rain event where the collection system does not have a large impact on the studied flood situation, that is rain events with long return period of 100 years or more (MSB 2013).

The accuracy of the calculations in the model are dependent on the resolution of the elevation model and the size of the computational grid. In urban areas, it is not recommended to use a computational grid larger than 4 by 4 m. This is so structures are depicted correctly, especially since surface roughness heavily affects surface runoff (MSB 2017). With lower resolution there is a risk that the flood extent is wider and result in lower water depths. Calibrating the model is

another important factor for accuracy. Calibrations can be done by altering the model parameters so that the result from the model corresponds to experimental values taken in the field. When modelling extreme scenarios, calibrations are difficult since there is often no observations of flooding distribution or measurements of or water depths or water flows. Infiltration capacity is therefore the most crucial parameter for runoff events (MSB 2017).

1.8 IMPORTANCE OF ANTECEDENT CONDITIONS

Both in reality and in flood modelling, the antecedent soil moisture conditions regulates the proportion of rainfall that infiltrates versus becomes surface runoff (Saleh 2021). During a rain event the infiltration rate of the ground slows as rainfall continues. When the ground becomes more saturated, the surface runoff increases and therefore also the magnitude of the flooding. If the ground is fully saturated at the beginning of a rain event, all rainfall will become runoff (Environment Agency 2019). It is not only antecedent rainfall events that affect initial soil moisture conditions in flood modelling, but baseflow conditions, snowmelt, and watershed characteristics. It is a complex system, and all factors impact the severity of flood risk. Very dry or compacted antecedent soil conditions can also be a risk. Parched or compacted soils may hinder infiltration from rainfall and are therefore more prone to runoff (Saleh 2021).

1.9 2D OVERLAND MODELLING IN MIKE+

MIKE+ is the latest software developed by DHI (Danish Hydrological Institute) and consists of multiple modules depending on purpose of modelling and is a tool commonly used by MSB for cloudburst modelling (MSB 2014). The 2D Overland module used for this thesis enables, amongst other things, 2D modelling of free-surface flows, pollution transport and coupling with 1D collection system networks. The module uses DHI's 2D engine MIKE 21 FM and solves the two-dimensional St. Venant equations for dynamic flow (DHI 2023b).

The basis for constructing a model in 2D Overland is defining a 2D model area which is called bathymetry in MIKE+. In this thesis, the bathymetry will be called elevation model to avoid mix up with the term for study of beds of water bodies. The elevation model is a computational grid or mesh, and the type can be either flexible or rectangular. Rectangular grid consists of uniformly-spaced, orthogonal grid points which represents the domain while flexible is non-uniform and can consist of triangular elements, all representing the model domain (DHI 2023a). More simply expressed, the elevation model in this study is a 2D rectangular grid expressed in x- and y-direction containing elevation data for each cell. The defined 2D domain may be open or closed. If the boundary is closed, there is no flow across the domain border while open boundary allows flow (DHI 2023a).

Initial values for the hydrodynamic variables for the 2D domain can be either dry domain, varying in domain or uniform water level. When specified as dry, the water depth and velocity across the domain will be zero at the start of the simulation. Uniform water level consists of a single value of water level across the domain. Cells within the areas where topography is higher than the single value will be dry at the start of the simulation. Varying in domain means spatial variation of the initial condition within the model area and may be defined, similarly to the elevation model, with a 2D grid file (DHI 2023a).

Wetting depth (h_{wet}) and drying depth (h_{dry}) are threshold values used to classify elements (cells) into dry, partially dry or wet elements during overland computations. These classifications are used to identify flooded boundaries which then determines which elements to be included in calculation of flux. A condition is that wetting depth must be larger than drying depth (DHI 2023a).

There are multiple options to specify surface roughness of the 2D domain: uniform, varying in domain, varying in domain and time or varying in domain and flow dependent and can either be expressed in Manning's number (M or n) or Chezy's number (N). Uniform is a single value for the whole domain while varying in domain/domain and time is defined with a 2D grid file. Flow dependency adds an option to defining Manning's number as a function of water depth or flux or as a roughness curve (DHI 2023a).

Similarly, to surface roughness there are multiple options to define the precipitation and infiltration throughout the simulation. Precipitation can be none, constant or varying in domain and time. The infiltration can be varying in domain varying in domain and time/flow dependent and using capacity. Varying in domain indicates a spatial variation and varying in time a temporal variation (DHI 2023a).

The 2D Overland module uses a self-adapting time step for the numerical solution. This means that the time step is automatically adjusted based on current conditions, if changes in these conditions happens rapidly the time step will decrease and vice versa. Using the self-adapting time step optimizes simulation times and the stability of the model (DHI 2023b).

1.10 AIM AND OBJECTIVES

The aim of this thesis is to explore, using MIKE+, if usage of different soil types in urban green areas can mitigate urban pluvial floods and determine the importance of antecedent conditions. The soil types investigated in this thesis is sandy loam, silt, and clay. Two-dimensional surface runoff models of two different urban catchments, varying in percentage of green area within the model area, will be forced with 100-year storm event with varying soil type and antecedent soil moisture content for all green areas. Both model areas are defined by their catchment boundary and all urban green areas within the boundary will be assumed to be grass covered. The objective is to examine the hydraulic response when varying soil characteristics affecting infiltration.

The aim is to be fulfilled by answering following research questions:

- How do soil type and antecedent soil moisture content affect:
    - Flood extent?
    - Maximum flood depth?
    - Overland flow?
    - Maximum discharge, time to reach peak and cumulative discharge from the catchment?
- Is antecedent soil moisture content critical in floods?

1.11 DELIMITATIONS

The scenario in this thesis assumes that the capacity of the drainage system has been reached and therefore the models will be constructed without it. Due to lack of observations the models will not be calibrated. Alterations deviating from real conditions in the model areas will be made, both models may therefore be considered synthetic model areas.

2 METHOD

2.1 URBAN AREAS AND SOIL TYPOLOGIES

In this study, three different soil types were chosen to represent the soil in all green spaces in the model area. The two conditions for all soils were that they were suitable for growing a lawn and could be found in the soil texture triangle. The wanted outcome was to find one common soil type used in urban green spaces in Sweden and two "extreme" soils. One of the soil types

were chosen on recommendation by AMA Anläggning 20, a work of reference when constructing soil beds. For "normal" executions, the reference stated a span of requirements for soil texture distribution (Svensk Byggtjänst 2020). The minimum requirements of textural distribution resulted in a soil mixed with different sizes of gravel. One condition for the soil was that it was included in the soil texture triangle and since gravel is not part of the texture triangle it was not an option. Instead, the maximum requirement of textural distribution was chosen which resulted in one soil being classified as sandy loam. The two other soils were chosen as extreme soils, meaning that soil texture should contain as much of either clay, silt or sand as possible but still be able to grow a lawn. To find extreme soils, a literature study was conducted to obtain experimental texture data of soil samples taken from lawns globally, since there were no studies to be found on lawns in Sweden. The literature study resulted in the choice of clay and sand. See Appendix B, Table 9, for soil texture and sources.

Since either of the experimental data sets contained all necessary data to run the models, Tyréns provided data from a database they have created with hundreds of different soil types extracted statistically random from the soil texture triangle. From this database, the three soils in Table 2 where chosen, being the ones closest to the textural distribution of the soils found through the literature study.

Table 2. Soil type and textural distribution for chosen soils shown in a percentage of sand, silt and clay.

Soil type	% sand	% silt	% clay
Sand	88	5	7
Sandy loam	62	24	14
Clay	24	16	60

2.2 MODEL AREAS

For this thesis two different study areas were chosen, Fagersjö and Farsta-Larsboda, both located in suburban areas south of Stockholm city. The model boundary for each area were the catchment boundary and since both catchments had outlets in lakes the catchment areas were extended over the lakes for modelling purposes. Farsta-Larsboda was suggested as a model area since there was already a MIKE+ model for the catchment constructed by Tyréns. Fagersjö was chosen as due to the large portion of green areas within the catchment boundary, in contrast to Farsta-Larsboda which had large built-up areas. Larger built-up areas both increases the runoff speed due to more surfaces with lower roughness and there are more places within the catchment that can entrap water. In Figure 2 a map of Sweden and Stockholm shows the location of these catchments. Figure 3 shows an orthophotography of model areas including the surface roughness with Fagersjö to the left in the figure and Farsta-Larsboda to the right. The total model area of Fagersjö was 0.825 km^2 and 1.64 km^2 for Farsta-Larsboda. If solely looking at hardened versus non-hardened surfaces (disregarding the lake within the model areas) Fagersjö catchment had 84.4 % of green area while Farsta-Larsboda had 57.3 %.

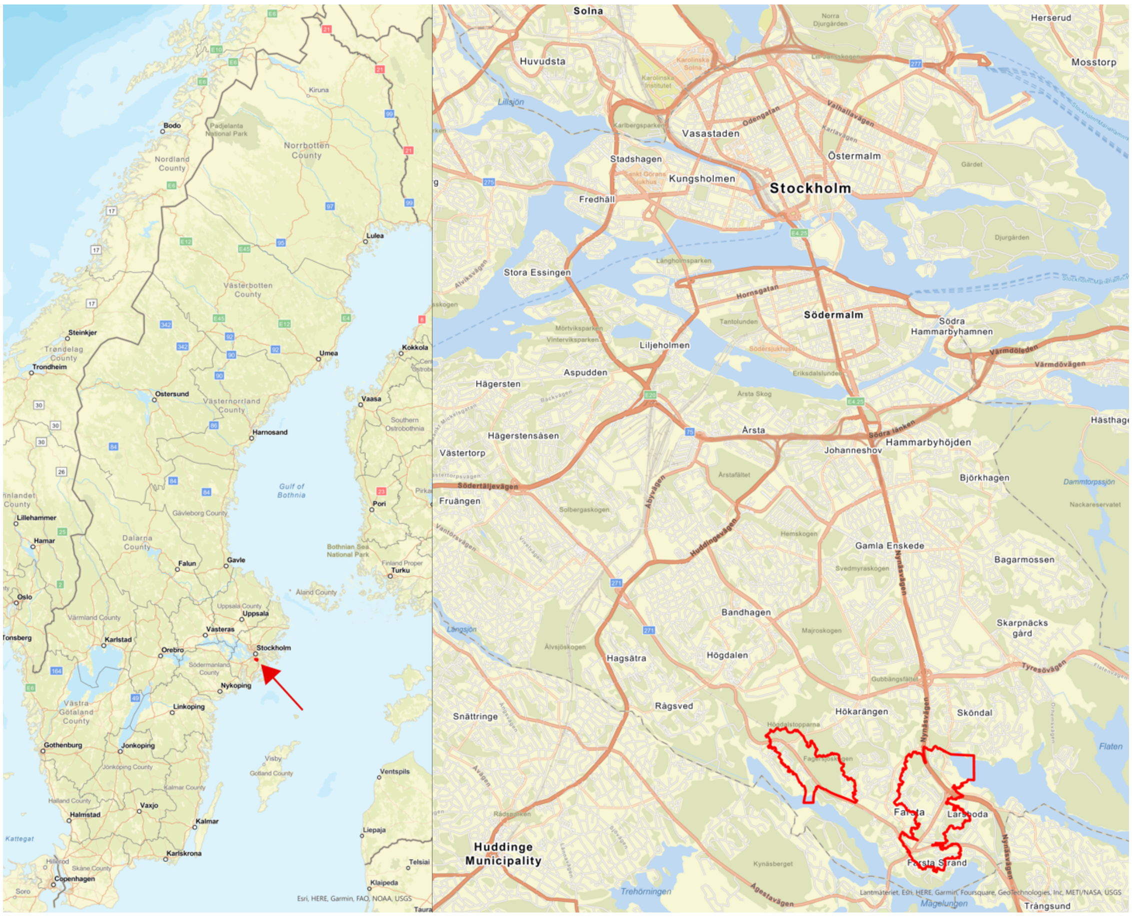

Figure 2. Location of catchments. Map of Sweden showed to the left and a map of Stockholm to the right in the figure. The marked red areas represent Fagersjö catchment (left) and Farsta-Larsboda (right).

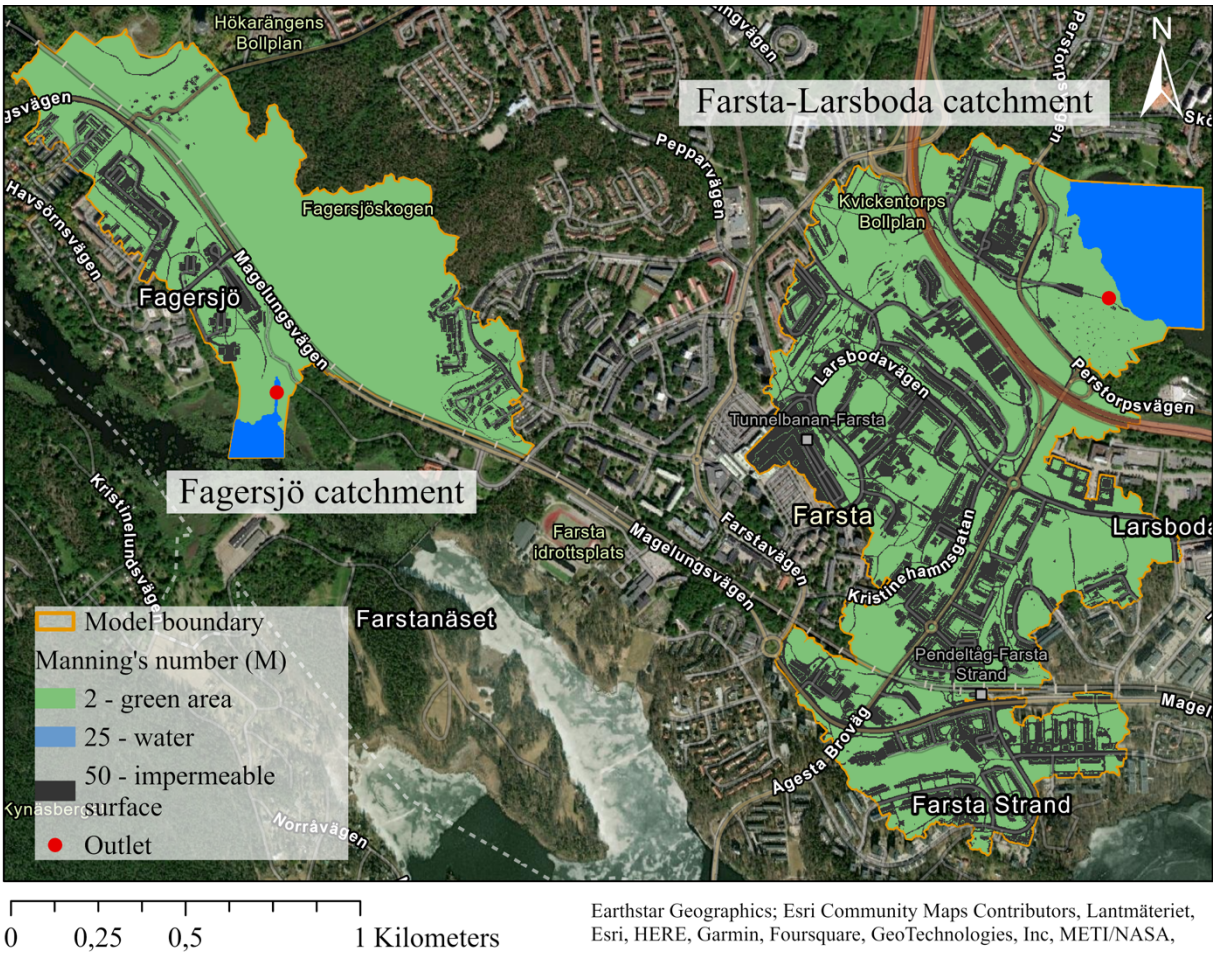

Figure 3. Model areas of Fagersjö and Farsta-Larsboda catchment. Outlet indicates where the catchment ends and empties into lake. The colours green, blue and black represent the different surface roughness within the model area expressed as Manning's number (M) in $m^{(1/3)}/s$.

Simplifications of reality had to be made to construct a 2D surface runoff model of the catchment area. As Figure 3 shows, both Fagersjö and Farsta-Larsboda have areas with forest. These were all assumed to be lawns with the same soil type and properties and therefore also same Manning's number as all other green areas within the catchment. All other surfaces were assumed to be impervious surfaces (roads, rooftops etc.) with same Manning's number. Because of this, the model areas can be seen as synthetic model areas since they do not correctly depict the actual suburban areas.

2.3 MODEL SET-UP

To build a model in MIKE+ requires data and processing of this data to some extent. The already built model for Farsta-Larsboda only needed a few alterations to have the same conditions as the Fagersjö model, therefore the sections below describe how the Fagersjö model was set up, but generally they had the same methodology for construction and same input parameter values were used.

2.3.1 2D Domain

The topography of chosen model area is defined as bathymetry in MIKE+. This data was collected from SCALGO Live, a software that offers country specific elevation models, multiple analysis of for example sea-level rise and building footprints amongst other things. The elevation model of Sweden they offer is primarily based on data from Lantmäteriet (Scalgo

Live 2023). By using the SCALGO Live watershed function, the catchment of Fagersjö could be identified and a DEM (digital elevation model) was obtained for the model area. The resolution of the DEM was 1x1 m with coordinate system defined as SWEREF99 18 00 (specific for that part of Sweden). The elevation model was then processed in ArcGIS PRO (version 2.9.5) and defined by using the catchment as a boundary for the model area. All cells remaining outside of the catchment boundary was assigned "true land values" which enclosed the model domain. In the model, this was defined as a closed 2D boundary condition. Both catchments had outlets in lakes and therefore the model area was extended beyond the actual catchment area. In the elevation model files, the elevation for the cells containing catchment outlet (lake) were lowered with roughly 1 m. A replica of the elevation model files was then created with actual water level in the lakes. This was added as an initial condition for the model. The outlet border remained open to ensure a water flow out from the model which was defined as a 2D boundary condition with constant water level.

The elevation model was then compared with a current orthophotography of the model area and a dataset of culverts in the area from Trafikverkets Lastkajen was added to locate possible flow paths or obstacles for flow paths that was missing from the model. No alterations were needed. The DEM only contained elevation data of the terrain and therefore buildings in the model area had to be added so that water did not flow over the buildings. The building footprint data set was also obtained as from SCALGO Live with data from Lantmäteriet and converted from a vector format to a grid format in ArcGIS PRO. The buildings were then added to the DEM by raising all cells containing buildings with 2 m. Elevation model for both model areas can be seen below in Figure 4.

To lower computational times the resolution for the grids for both models were resampled from 1x1 m to 2x2 m.

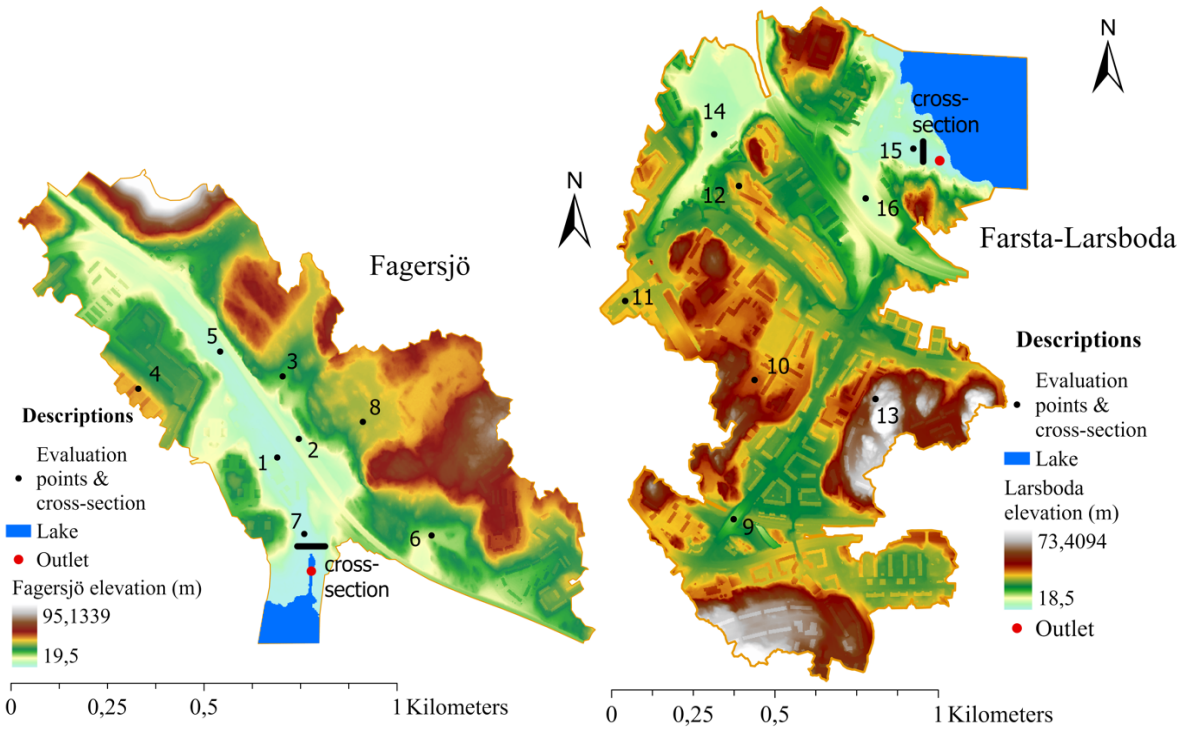

Figure 4. Elevation model for Fagersjö catchment seen left in figure and Farsta-Larsboda to the right. Numbered points are chosen evaluation points and the cross-sections are upstream the catchment outlet. The red circle shows a part of the catchment outlet. Note that the evaluation points are not true to size

2.3.2 Wetting and drying

The model values for wetting and drying depth were set to 3 mm and 2 mm based on recommendation by Tyréns.

2.3.3 Surface roughness

Information on land cover for the model area was obtained from SCALGO Live and processed in ArcGIS PRO by converting the vector format into a grid format. By comparing an orthophotograph of the model area with the data from SCALGO Live a few alterations was made after detecting some roads and buildings missing in the data set. As mentioned earlier in the thesis, an assumption made for both model areas were that all impervious areas had the same Manning's number, and all other areas were assumed to be green areas with homogenous properties and therefore also same Manning's number. Values for surface roughness was chosen based on the recommendation from MSB: Manning's number 2 for green areas and 50 for impervious areas as seen in Table 1. Since both Fagersjö and Farsta-Larsboda catchment had outlets in lakes a third Manning's number, 25, was added for water based on recommendations from a modeller at Tyréns. A map of surface roughness distribution in both areas can be seen in Figure 4. Due to instability issues during test runs of the Fagersjö model all adjacent cells with an elevation difference causing an angle larger than 45° was given a Manning's number of 2, regardless of prior Manning's number.

2.3.4 Infiltration and antecedent soil moisture

Infiltration data was provided by Tyréns (in preparation) in the form of infiltration curves for clay and sandy loam with three different antecedent soil moisture contents, and a constant value for sand. The infiltration curves and infiltration rate for sand are derived from modelling in Hydrus 1D, a modelling environment that can be used for simulating movement of water in variably saturated media (USDA 2020). These simulations were conducted independently of this thesis. A brief description of Tyréns method can be seen in Appendix C. In Hydrus 1D, the antecedent soil moisture is a function of capillary pressure which varies with depth and is therefore not directly translatable to a certain value. Instead, the antecedent soil moisture content for each soil type is represented by the percentile from approximately 280 datasets for each soil type, 5^{th} being low antecedent soil moisture from the dataset, median being 50^{th} percentile and 95^{th} being high moisture content. An example of an infiltration curve can be seen in Figure 5. The blue circles in the graph are results from the simulations in Hydrus 1D and represents infiltration rate over accumulated rain depth and the red line the interpolated curve. The resultant equation for I, infiltration rate over accumulated rain depth, for each soil and antecedent soil moisture was obtained from can be seen in Table 3.

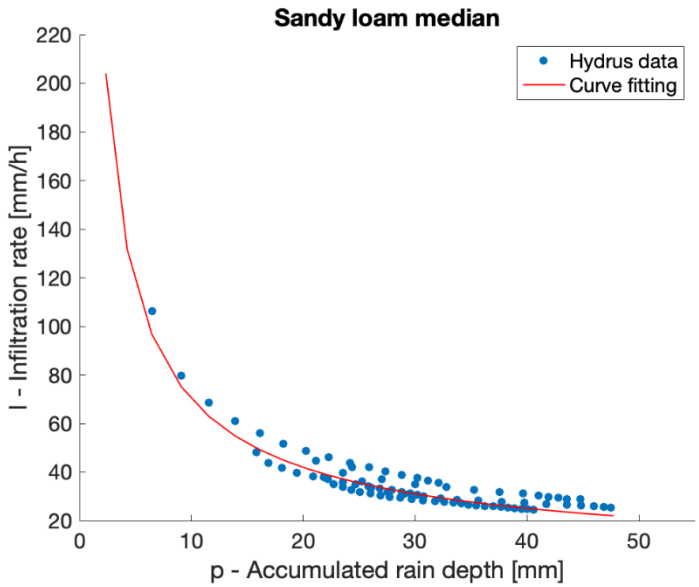

Figure 5. Curve fitting by interpolation. The blue circles represent results from Hydrus 1D simulations and the red curve is the interpolation.

Table 3. Infiltration curves for the soils, obtained from Tyréns.

Soil	Soil moisture	Equation	Start value
Sandy loam	5th	$I = 783.95 \cdot p^{-0.89}$	9 mm
	median	$I = 384.94 \cdot p^{-0.74}$	7 mm
	95th	$I = 228.3 \cdot p^{-0.62}$	7 mm
Clay	5th	$I = 7.27 \cdot p^{-0.37}$	2 mm
	median	$I = 6.98 \cdot p^{-0.38}$	2 mm
	95th	$I = 4.97 \cdot p^{-0.34}$	2 mm

To integrate the fitted curve into MIKE+, two different infiltration types in MIKE+ 2D infiltration editor were used. For sandy loam and clay the infiltration type was set to varying in domain and time. This implies that the net infiltration rate in all green areas during the precipitation event vary both spatially and temporally. To use this function one grid series file was needed and one time series file. The grid series file held information on which cells contained impervious versus pervious surfaces. The time series gave temporal information of infiltration rate for the pervious surfaces.

Firstly, rain intensity (mm/h) from the generated CDS (more information in section 2.3.5 below) was converted to rain (mm) for each 5 min interval in the time series. The rain was then re-calculated to accumulated rain (mm) for the time steps in the interval which equals to the parameter p in the equations in Table 3. To obtain data series for infiltration over time, I, the equations in was used. Since the data series only included two hours of rain, the remaining two hours of the simulation the infiltration rate was assumed to be constant using the final value in the data series. As seen in Figure 5, the data points (in blue) do not start at zero. Between zero

and the first data point, the infiltration was assumed to be constant using the given value at the same rain depth (mm) as the datapoint corresponds to.

To derive infiltration curves from these simulations to use as input in MIKE+ there was a condition that the simulation generated runoff. For sand, none of the simulations from the Hydrus model generated any runoff (all rain was infiltrated) and it was therefore not possible to obtain any infiltration curves. Instead, a constant infiltration rate from the Hydrus 1D simulations was used of 97.5 mm/h. The infiltration type in MIKE+ 2D infiltration editor was therefore set to constant and only a grid series file containing information on infiltration rate for all pervious surfaces was needed, all impervious surfaces was set to 0 mm/h.

2.3.5 Precipitation

To generate a 100-year storm event, the software *CDS_regn* developed by Tyréns was used. The software uses Dahlström's formula as seen in equation 1 and creates a CDS with given return period. Other parameters for the calculations are desired time step of blocks, length of central block, r-value and time centring of rain which indicates when half of the rain duration should occur. Parameters and corresponding value can be seen in Table 4.

Table 4. Parameters used to generate CDS.

Parameter	Value
Rain duration T_r (min)	120
Time step (min)	5
Central block (min)	10
r-value	0.37
Time centering of rain	10
Return period F	100

The generated CDS had a simulation time of 4 hours and a rain duration of 2 hours. The two hours without rain were at the end of the simulation to give time for all precipitation to accumulate in the model and to ensure that maximum flow at the outlet was reached.

2.3.6 Simulation length and time step

The 2D Overland module uses a self-adapting time step. Default values of minimum and maximum timestep of 0.01 sec and 10 sec was therefore used. The length of the simulation is dependent on simulation time of the CDS rain (in this thesis 4 hours). There is also an option to alter the critical CFL number (Courant-Friedrich-Lévy) which determines the size of the time step needed to keep stability in the model. Recommended value by DHI is between 0 and 1, altering it from default is less important since the time step in MIKE+ 2D Overland is self-adapting (DHI 2023c). Default value of 0.8 was chosen.

2.4 OUTPUTS

To investigate how different soil types and antecedent conditions in urban green areas affect the hydraulic output in the urban areas when simulating a 100-year storm a few different outputs was wanted.

Some outputs were default, such as statistics where maximum water depth (m) for each cell was given. Some had to be specified, such as water depth (m), current speed (m/s), Q flux ($m^3/s/m$) and P flux ($m^3/s/m$). All the specified outputs present the calculated value for each grid cell at every time step throughout the simulation. It can be described as each time step has a "layer" of data. Q flux and P flux gave the flux in x- and y-direction and together with water depth it was possible to calculate discharge (m^3/s) and cumulative discharge (m^3/s) for wanted cross-sections at the outlet of the model areas. The "layers" for water depth and current speed could be multiplied and later used to calculate runoff in the cells.

2.5 EVALUATION POINTS AND VARIABLES

The evaluation variables chosen for this thesis was percentage of flooded model area, peak discharge at catchment outlet, time to reach peak discharge and cumulative discharge and for chosen evaluation points investigate maximum flood depth and surface runoff. All cells (disregarding cells at outlet/lake) with a maximum flood depth larger than 0.15 m at any time step was considered flooded. This threshold was chosen on the likelihood of causing property flooding in some areas (Environment Agency 2019). Maximum flood depth was also an evaluation variable for chosen evaluation points. In this case, the threshold was not considered. This was so a comparison between flood depth at the evaluation points could be made between usage of different soil type and varying antecedent soil moisture content. The evaluation variables for discharge were deemed a way to compare how much water from the catchment that reaches the outlet (does not infiltrate). The time to reach peak discharge may show indications whether that the infiltration caused a delay in peak discharge or not. To evaluate the flow upstream the catchment outlet, surface runoff was calculated for the evaluation points.

The evaluation points mentioned above were one grid cell (2 by 2 m) and to select location for these points in the model areas the following criteria were set up that was deemed especially significant:

- Flooding occurs at the evaluation point some point throughout the simulation (no threshold)
- Some variation of high and low runoff
- Include low point in each model
- One evaluation point close to outlet (upstream)
- Focus on pervious areas but add at least one impervious in both models
- Some spatial distribution of evaluation points within the model area
- The evaluation point should not be affected by any outlet errors
- If possible, one evaluation point in each model were to be at place of critical infrastructure or vital societal functions

To determine the location of these points, one trial simulation in each model was conducted to obtain results of runoff and maximum flood depth. These results were used to create to map layers in ArcGIS and from these locate evaluation points based on the criteria above. Besides the outlet cross-section in both model areas, a total of 16 evaluation points were chosen, 8 in each model. A full list of evaluation points, their manning's number and coordinates can be seen in

Table 5 below. Elevation model for Fagersjö catchment seen left in figure and Farsta-Larsboda to the right. Numbered points are chosen evaluation points and the cross-sections are upstream the catchment outlet. The red circle shows a part of the catchment outlet. Note that the evaluation points are not true to size and to see placement within the model area, see Figure 4.

Table 5. Manning's number and coordinates for valuation points and cross-section in both model areas.

		Coordinates (SWEREF 99 00 18)	
PointID	Manning's number M ($m^{1/3}/s$)	x	y
1	50	153745	6570179
2	2	153801	6570227
3	2	153759	6570389
4	2	153385	6570357
5	50	153597	6570453
6	2	154145	6569977
7	2	153815	6569981
8	2	153967	6570271
Cross-section (Fagersjö)	2	153797-153869	6569949
9	50	155585	6569057
10	2	155649	6569483
11	50	155253	6569725
12	2	155601	6570077
13	2	156019	6569425
14	2	155525	6570235
15	2	156135	6570191
16	2	155989	6570039
Cross-section 2 (Farsta-Larsboda)	2	156165	6570151-6570213

2.6 PROCESSING OF RESULT DATA

The result data was processed directly in MIKE+, MIKE Zero, excel and MATLAB were used for data analysis. The descriptions below describe how data was processed from each simulation.

To calculate percentage of flooded model areas and extract maximum flood depth in the evaluation points the output "maximum water depth" was used. The data was transferred to an excel sheet that extracted the maximum flood depth in each evaluation point by finding the given pointID and returning the value for maximum flood depth in that point. The excel sheet also returned the number of cells with a flood depth larger than 0.15 m. To obtain the percentage of flooded model area, Equation 2 was used.

$$\%\ flooded\ model\ area = \frac{No.\ cells_F}{No.cells_T - No.\ cells_{\frac{O}{L}}} \cdot cell\ area\ \cdot 100 \qquad (2)$$

where No. $cells_F$ represent the number of cells with maximum flood depth larger than 0.15 m, No. $cells_T$ is total amount of cells in the whole model area which is subtracted by the No. $cells_{O/L}$ that contained outlet/lake. The cell area is the size of a grid cell which was 2 by 2 meters. Same excel sheet was used to extract the maximum flood depth for each evaluation point.

For surface runoff at the evaluation points, the outputs water depth (m) and current speed (m/s) was utilized. Firstly, the two outputs were multiplied which resulted in a grid file with flux

($m^3/s/m$). This was transferred to MIKE Zero where it was possible to extract the data series over time for each evaluation point by putting in the x- and y-coordinates for the location. The data series was then extracted into an excel sheet and multiplied with cell width (2 m) to obtain the surface runoff (m^3/s) over time.

A time series for discharge at catchment outlet was calculated in MIKE Zero by transferring an output grid file containing water depth, Q-flux and P-flux for each time step in the simulation (see section 2.4 for more details on output files). By putting in the start and end coordinates for the cross-section, MIKE Zero returned a data series containing discharge and cumulative discharge over time and from that it was also possible to obtain time to reach peak discharge.

3 RESULTS

3.1 PERCENTAGE OF FLOODED MODEL AREA

To determine the flood extent in the model area, the percentage of flooded cells was determined and then recalculated to a percentage of the whole model area. A deduction was made for all cells containing outlet/lake. If the flood depth exceeded 0.15 m at any point throughout the simulation the cell was considered flooded. The results can be seen in Figure 6 where each soil type and antecedent soil moisture for both model areas can be seen individually (95th being the highest soil moisture and 5th being the lowest from the Hydrus 1D simulations).

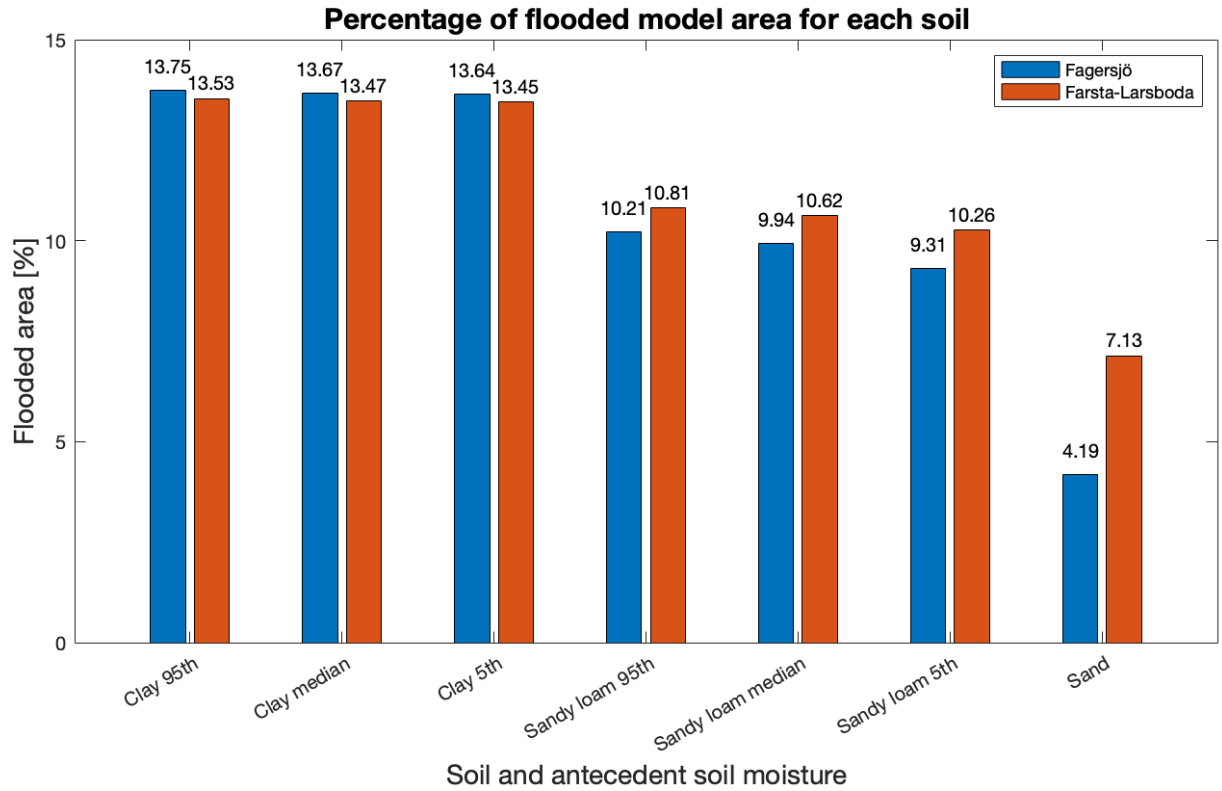

Figure 6. Percentage of flooded model area for both catchments sorted in highest percentage to lowest in each catchment, Fagersjö shown in blue and Farsta-Larsboda in red.

All simulations in both model areas showed in the same result pattern, increased flood extent with increasing antecedent soil moisture and decreasing infiltration capacity. In Fagersjö catchment, if a mean of the results with clay is calculated, the difference between the usage of clay and sand is 9.5 % for flooded model area. The mean can be seen as a more representative result to use for comparison since sand does not have three different antecedent conditions. For

Farsta-Larsboda the difference is 6.35 %. If all green areas were to be of the AMA recommended soil type sandy loam the difference in Fagersjö model would be 3.87 % less flooded area compared to a mean value of clay and 5.63 % more than sand. In Farsta-Larsboda the flooded area would decrease with 2.92 % in comparison with clay and increase with 3.43 % when compared to the usage of sand in all green areas. The largest difference in percentage flooded area for when comparing antecedent soil moisture is for sandy loam 95th and sandy loam median. In Fagersjö catchment the difference is 0.9 % and 0.55 % in Farsta-Larsboda. For clay, the difference is 0.11 % and 0.08 % respectively.

3.2 MAXIMUM FLOOD DEPTH AT EVALUATION POINTS

To obtain a more in-depth analysis of the pluvial flooding in both model areas, 16 evaluation points were selected (eight in each model area). The maximum flood depth at these locations for all simulations can be seen in Figure 7 for Fagersjö and in Figure 8 for Farsta-Larsboda. The different coloured dots in the plots each represent the soil and antecedent condition used for that simulation. For this analysis, the chosen threshold of 0.15 m for a flooded cell was not used.

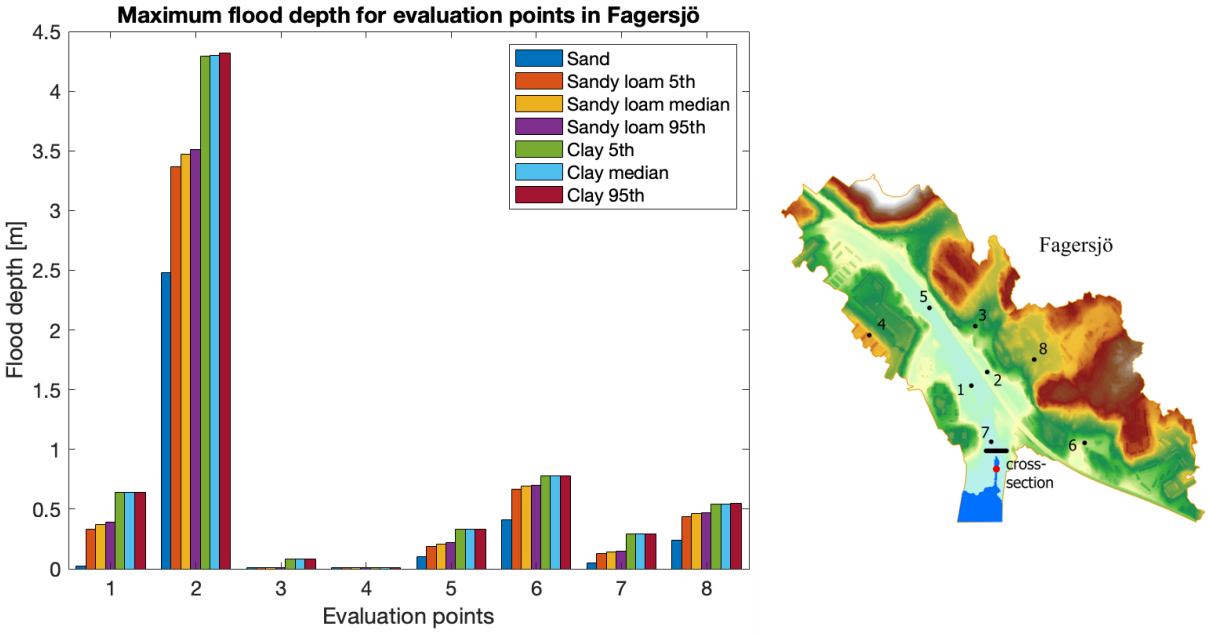

Figure 7. Flood depth at evaluation points 1-8 in Fagersjö. Each colour represents a soil type and corresponding antecedent soil moisture. Placement for evaluation points can be seen to the right in the figure.

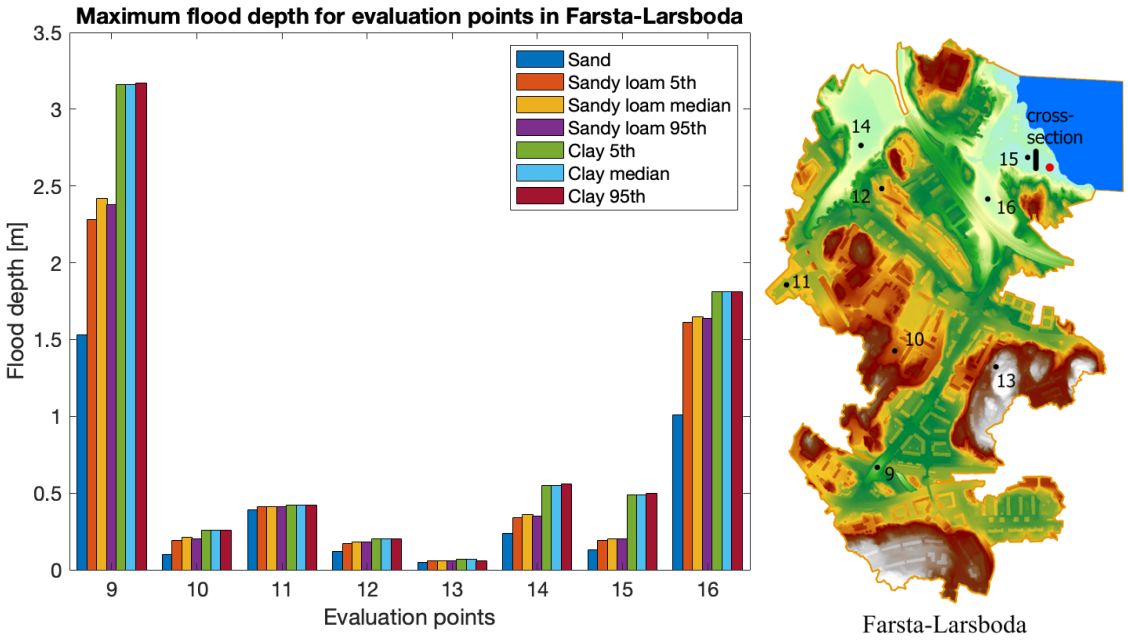

Figure 8. Flood depth at evaluation points 9-16 in Farsta-Larsboda. Each colour represents a soil type and corresponding antecedent soil moisture. Placement for evaluation points can be seen to the right in the figure.

Most evaluation points showed the same result pattern, the soil type with lowest infiltration capacity and highest antecedent soil moisture resulted in largest maximum flood depth. The largest difference in maximum flood depth between the different scenarios is in evaluation point 2, 9 and 16 being 1.80 m, 1.64 m and 0.800 m when comparing mean maximum flood depth for clay and sand. The smallest differences in maximum flood depth are found in evaluation point 4, 3 11 being 3.40×10^{-4} m, 75.0×10^{-4} m and 280×10^{-4} m. The largest differences found between antecedent soil moisture content was at evaluation point 2 in Fagersjö, 0.14 m difference between sandy loam 5th and 95th and evaluation point 9 in Farsta-Larsboda, 0.14 m between sandy loam 5th and median.

3.3 OVERLAND FLOW AT EVALUATION POINTS

In the same evaluation points where maximum flood depth was investigated, surface runoff was calculated. Below is a selection of plots presenting surface runoff over time for each scenario with corresponding time to peak and maximum runoff. The color represents soil type, and the marker indicates the antecedent soil moisture of the soil. S is the abbreviation for sand, C for clay and SL for sandy loam. Runoff at evaluation points with impervious surface was deemed a less significant result. This was because surface runoff at these locations did not directly occur due to saturated soil but indirectly from saturated soil in nearby areas upstream. Remaining plots can be seen in Appendix D (Figure 17, Figure 18, Figure 19 and Figure 20) which also includes maximum surface runoff and time to peak for all evaluation points (see Table 10). Note that the simulation starts at 00:05, this is to avoid model instabilities, and after 2 hours into the simulation the rain event has finished. Between 00:45-00:50 the rain intensity of the CDS reaches its peak.

In general, the runoff at all selected evaluation points showed the same pattern. Maximum runoff increased with decreasing infiltration capacity of the soil and increasing antecedent soil moisture. For most of the evaluation points, time to reach peak runoff varied 0-5 minutes (one time step) between usage of different soil types and 0 minutes for different antecedent soil moisture content. Time of peak runoff was between 00:50 and 1:00 hours into simulation for

most evaluation points which is around the same time as the rain intensity from the CDS reaches its peak (00:45-00:50), with a slight delay in a few cases. The three evaluation points with time to reach peak overland flow that deviated from the general pattern was evaluation point 1 with peaks between 01:45-01:55 for sandy loam, evaluation point 7, see Figure 9, that reached peak at 03:00 for clay and evaluation point 15 with 02:20-02:25 for clay, see Figure 10.

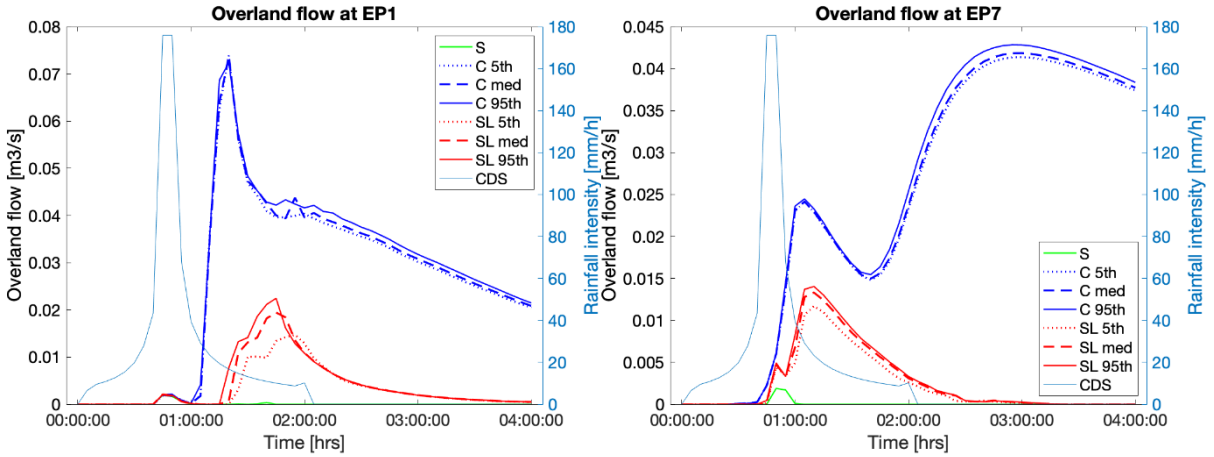

Figure 9. Overland flow at evaluation point 1 (left) and 7 (right). Different colours indicate different soil type and marker type different antecedent soil moisture. On the first y-axis, overland flow is displayed, on the second y-axis the rain intensity for the CDS is displayed.

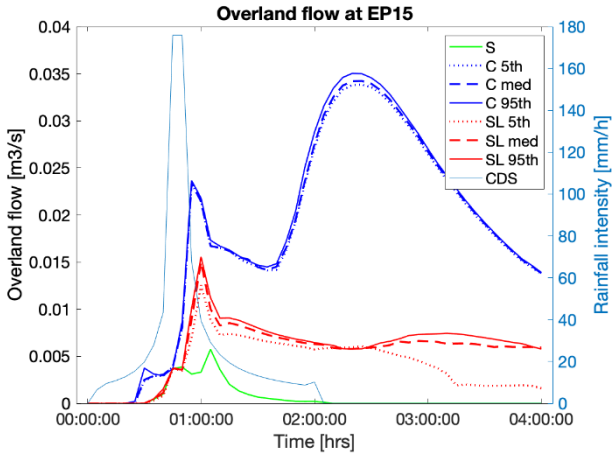

Figure 10. Overland flow at evaluation point 15. Different colours indicate different soil type and marker type different antecedent soil moisture. On the first y-axis, overland flow is displayed, on the second y-axis the rain intensity for the CDS is displayed.

Evaluation point 3 in Fagersjö catchment, see Figure 11, had the highest measured overland flow of 48.3×10^{-2} m^3/s for clay 95th. In that same evaluation point the lowest overland flow was 19.3×10^{-2} m^3/s with sand. In Farsta-Larsboda the highest measured overland flow (of pervious surfaces) was in evaluation point 16 with 12.63×10^{-2} m^3/s for clay 95th, also see Figure 11, and lowest 5.85×10^{-2} m^3/s with sand.

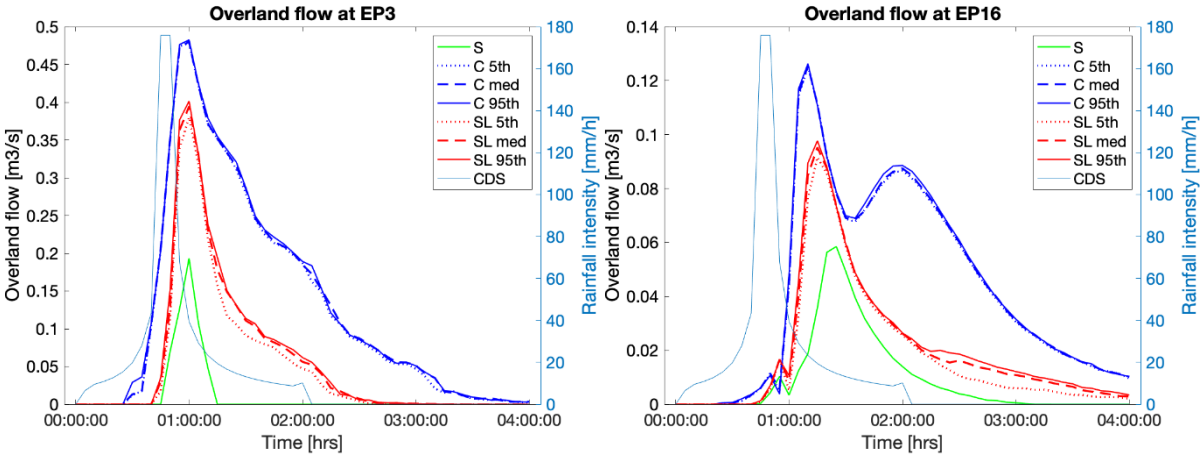

Figure 11. Overland flow at evaluation point 3 (left) and 16 (right). Different colours indicate different soil type and marker type different antecedent soil moisture. On the first y-axis, overland flow is displayed, on the second y-axis the rain intensity for the CDS is displayed.

The largest difference in overland flow measured for antecedent soil moisture content was found in evaluation point 6 between sandy loam 5th and 95th being 2.7×10^{-2} m^3/s, see Figure 12 below.

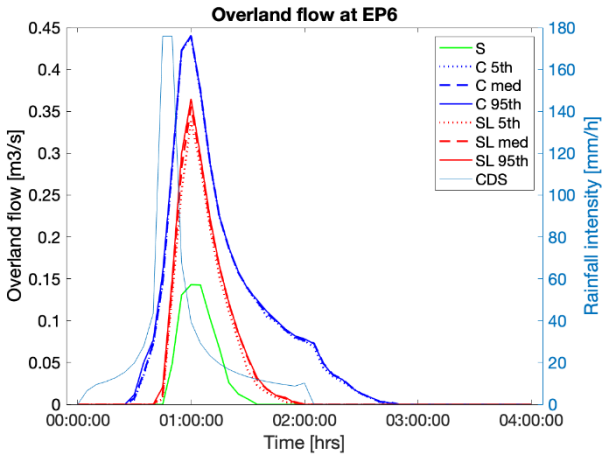

Figure 12. Overland flow in evaluation point 6 located in Fagersjö catchment. Different colours indicate different soil type and marker type different antecedent soil moisture. On the first y-axis, overland flow is displayed, on the second y-axis the rain intensity for the CDS is displayed.

Some evaluation points showed multiple peaks in surface runoff (EP 7, 13, 15 and 16), as seen in Figure 11 of evaluation point 16 in Farsta-Larsboda model. Evaluation point 4 in Fagersjö catchment did not generate overland flow in any of the simulations.

Two of the evaluation points had results deviating from the acknowledged pattern, evaluation point 13 and 9. These can be seen in Figure 13 below.

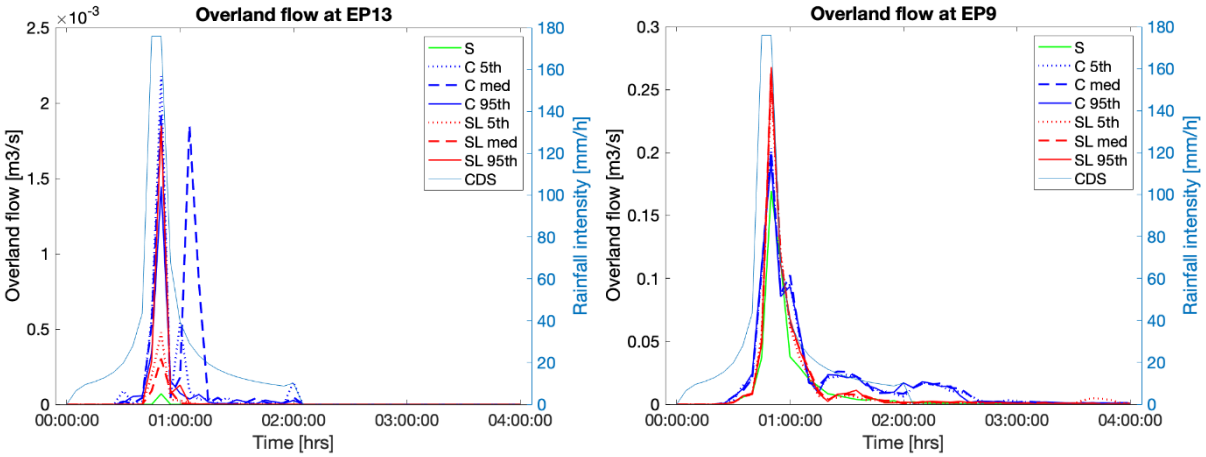

Figure 13. Overland flow at evaluation point 13 (left) and 9 (right). Different colours indicate different soil type and marker type different antecedent soil moisture. On the first y-axis, overland flow is displayed, on the second y-axis the rain intensity for the CDS is displayed.

3.4 DISCHARGE AT CATCHMENT OUTLET

In both catchments, a cross-section was created at the outlet to investigate surface runoff discharge out of the catchments. The results are presented below with a graph containing discharge throughout the simulation and tables with values for time to peak, maximum discharge and cumulative discharge. For both model areas, the result pattern continues that with decreasing infiltration of the soil and increasing antecedent soil moisture, the maximum discharge and cumulative discharge increases. There is only one exception for this result pattern. In Fagersjö catchment, clay 5th has a higher maximum discharge than clay median.

In Fagersjö catchment, seen in Figure 14, the time to reach peak discharge at the cross-section varies 0-5 min between the different scenarios. As mentioned above, there is a deviation in the result pattern, Clay 5th has 9.74×10^{-4} m^3/s higher maximum discharge compared to clay median but the total cumulative discharge for clay median is still higher which indicates that the discovered result pattern is still accurate.

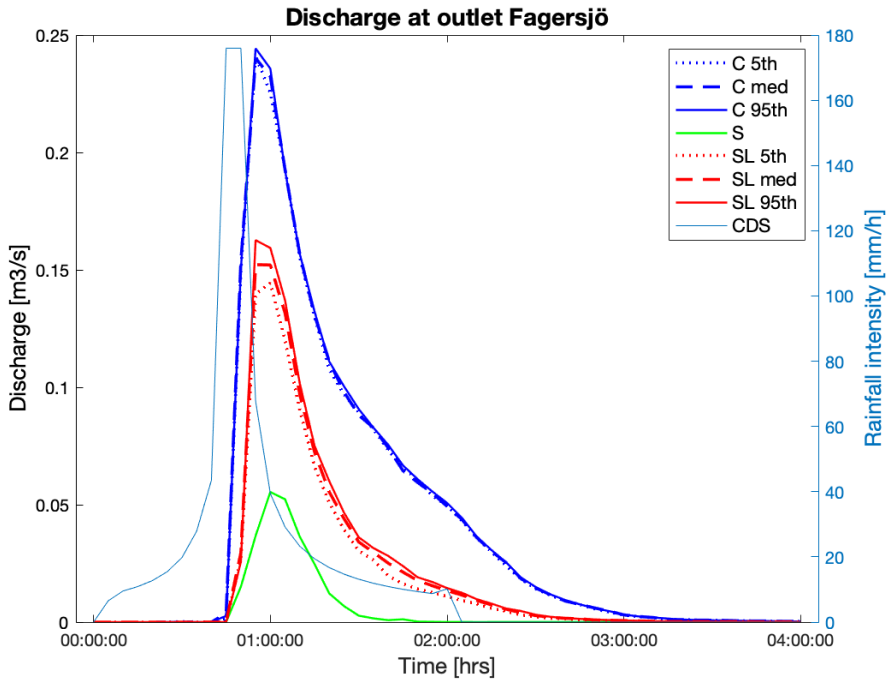

Figure 14. Discharge at the outlet cross-section in Fagersjö catchment. On the first y-axis, discharge at the cross-section upstream outlet is displayed, on the second y-axis the rain intensity for the CDS is displayed.

Table 6. Discharge at outlet in Fagersjö catchment.

Soil	Time to peak [hrs:min]	Maximum discharge [m^3/s]	Total cumulative discharge [m^3]
Clay 5th	00:55	0.241	598
Clay median	00:55	0.240	604
Clay 95th	00:55	0.244	610
Sand	01:00	0.055	74.3
Sandy loam 5th	01:00	0.144	255
Sandy loam median	00:55	0.152	283
Sandy loam 95th	00:55	0.163	298

When evaluating maximum discharge and cumulative discharge, which can be seen in Table 6 above, a mean value for clay and sandy loam is calculated since sand does not have multiple antecedent soil moistures. The largest difference occurs when comparing sand and a mean value of clay, the difference in maximum discharge is 0.186 m^3/s and for cumulative discharge the difference is 530 m^3. In the scenario where the soil type is sandy loam in all green areas the

maximum discharge decreases with 8.88×10^{-2} m^3/s and cumulative discharge with 326 m^3 when compared to clay and increases with 9.78×10^{-2} m^3/s and 204 m^3 in comparison to sand.

In Farsta-Larsboda, as seen in Figure 15, the discharge follows the same result pattern as Fagersjö but clay and sandy loam has two peaks and the maximum peak occurred later in the simulation, between 00:55 and 02:30. Time to peak did not vary between the antecedent soil moisture contents but maximum discharge did. It was consistent that maximum discharge and total cumulative discharge increased with increasing antecedent soil moisture content and with decreasing infiltration.

Table 7 below shows time to reach peak discharge, maximum discharge at the peak and cumulative discharge. The largest difference in maximum discharge and cumulative discharge is between sand and clay (also calculated from mean value), an increase with 1.31 m^3/s in maximum discharge and 9090 m^3 in cumulative discharge. If comparing sandy loam to clay the maximum discharge decreases with 1.14 m^3/s and 7460 m^3. When compared to sand the maximum discharge increases with 0.172 m^3/s and 1630 m^3.

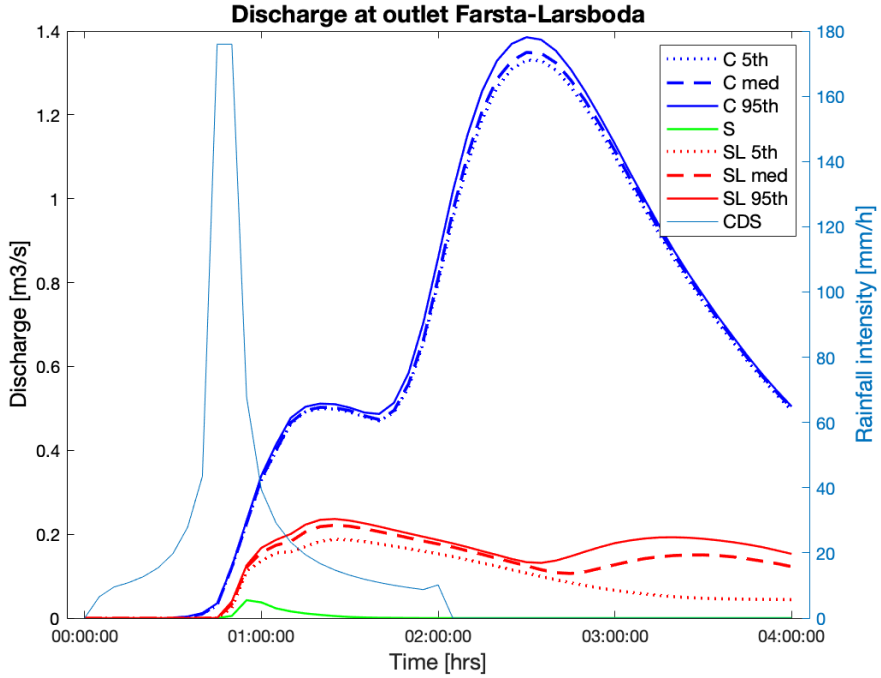

Figure 15. Discharge at the outlet cross-section in Farsta-Larsboda catchment. On the first y-axis, discharge at the cross-section upstream outlet is displayed, on the second y-axis the rain intensity for the CDS is displayed.

Table 7. Discharge at outlet in Farsta-Larsboda catchment.

Soil	Time to peak [hrs:min]	Maximum discharge [m^3/s]	Total cumulative discharge [m^3]
Clay 5th	02:30	1.33	8990
Clay median	02:30	1.35	9100
Clay 95th	02:30	1.39	9310
Sand	00:55	0.0428	46.7
Sandy loam 5th	01:25	0.188	1240
Sandy loam median	01:25	0.222	1760
Sandy loam 95th	01:25	0.236	2030

4 DISCUSSION

4.1 RESULTS OF EVALUATION VARIABLES AND POINTS

All results from all evaluation variables (percentage of flooded model area, maximum flood depth, overland flow and discharge) show the same pattern. The magnitude and extent of urban flood is dependent on soil type and antecedent soil moisture content. With decreasing infiltration capacity of the soil, sand having the highest infiltration capacity and clay the lowest, the flood extent, flood depth, overland flow and discharge at catchment outlet increases. This is consistent with the statement from Ren et al. (2020) with a grater infiltration rate and capacity, less surface runoff will be generated. Same pattern but reversed was found for antecedent soil moisture content. With increasing antecedent soil moisture flood extent, flood depth, overland flow and discharge at catchment outlet increases, but very low increase in comparison to altering soil type. These results were expected since the soil moisture content regulates the amount of water that can infiltrate a soil and infiltration highly affects surface runoff. When the soil is fully saturated, surface runoff is generated, and the flood depth will begin to rise in low points or points with no slope. Ahlmer et al. (2018) stated that multiple studies had concluded that the difference between minor and major flooding effects was dependent on antecedent soil moisture. This contradicts the findings in this study. Antecedent soil moisture content did affect the results but cannot be seen as the deciding factor on whether the flood consequences are major or minor. One possibility for this could be the return period of the rain event which affect amount of rainfall. The results from different antecedent soil moisture contents would likely vary greater if the return period was lower since more rain in relation to accumulated rainfall would infiltrate.

The results from percentage of flooded model area indicate that antecedent soil moisture content do have an impact on modelling flood predictions, but infiltration capacity is more critical due to the difference in flood extent between soil types. The results also shows that Fagersjö is more sensitive to changes in soil type and antecedent soil moisture content than Farsta-Larsboda which is shown by the larger difference in percentage of flooded model area. This is due to the high percentage of pervious surfaces within the model domain (84.4 % compared to 57.3 % in Farsta-Larsboda). When soil type varies, the infiltration rate varies and with larger areas of

pervious surfaces, it allows for more water to infiltrate. This also applies to antecedent soil moisture.

The maximum flood depth at the chosen evaluation points were difficult to visualise in a comprehensive manner due to the large difference in flood depth amongst the evaluation points causing datapoints for evaluation points with smaller variation in flood depth to overlap. All evaluation points showed a decline in flood depth when infiltration rate increased with change in soil type. When antecedent soil moisture decreased, so did flood depth as well except for evaluation point 13 where clay median caused higher flood depth than clay 95th. Considering a lower initial water content in the soil, this should not happen. The most likely explanation for this is a potential discretisation error in that location, which also would explain the deviating results for overland flow in the same evaluation point.

The evaluation points with highest flood depth, 2, 9 and 16, all having a flood depth greater than 1 m and evaluation point almost reaching 4.5 m with clay, were located in low points in the terrain causing the water to accumulate. Evaluation point 2 and 16 were located in deep ditches and evaluation point 9 in a viaduct. The deep flood depths in the ditches might not cause severe damage in a real storm event but having over 1.5 to over 3 m water in a viaduct may cause structural damage to the road and hinder rescue personnel from accessing certain aeras. A consequence that could be life threatening. This viaduct was investigated during the model setup to look for any constructions diverting runoff, but none was found. During the rain event in Gävle 2021, a viaduct was reported to have a flood depth of 4.5 m (Hallberg 2021). This rain event had a return period of 1000 years, not 100 years used in this thesis, but it still validates the possibility to reach this flood depth in viaducts. Another vital evaluation points is evaluation point 11, which is located at Farsta centrum, the town square with multiple stores and a shopping mall, all with entrances at ground level. If the simulated storm event would occur in reality, all stores would be flooded almost 0.5 m which could both cause structural damage and damage to goods.

A brief comparison of maximum flood depth and flood extent for sandy loam median was made with Stockholm municipality's cloudburst model's estimated maximum flood depth for Fagersjö and Farsta-Larsboda, see Appendix E, Figure 21 and Figure 22 (Stockholms stad 2023a). The Stockholm model was built in MIKE21 with a resolution of 4 by 4 m and five different surfaces with different Manning's (M): roads (70), green areas (5), roof (10), water (15), slope greater than 45° (2). The CDS was based on historical data from a rainfall in Copenhagen 2011 and had a return period of 100 years, duration of 6 hours, climate factor of 1.25, time step of 15 min and r-value of 0.5. There was also a deduction made for the storm water collection system (Thurin et al. 2018). The maximum rain intensity was 205.9 mm/h for 30 minutes. To represent infiltration, the built in infiltration module in MIKE21 was used and green areas were divided into four types with different infiltration properties. The infiltration also took antecedent moisture content into account (Thurin et al. 2018).

The results from both models are similar but it is difficult to draw an in-depth conclusion from the comparison since Stockholm municipality's model classify all flood depths larger than 1 m with the same colour and it is not possible to see exact flood depth (Stockholms stad 2023a). From a visual inspection, the Fagersjö model in MIKE+ appears to have a slightly larger flood extent than Stockholm municipality's model. Farsta-Larsboda is more difficult to compare because some areas in the MIKE+ model have greater flood extent than Stockholm municipality's model while other areas do not. The CDS used in the Stockholm model had greater intensity and duration. Based solely on this, it should result in greater flood extent and flood depth than the results in this thesis. Flood extent may differ due to the usage of different Manning's number and since the roughness of the surface affects both route and distribution

this could be one cause for the difference, especially in Farsta-Larsboda which had more impervious surfaces.

The differences in infiltration would also cause different results. The Stockholm model used constant infiltration while the models in this thesis only had constant for sand, for sandy loam and clay infiltration curves was used. Both models took antecedent conditions into account but used different methods and therefore not directly comparable. It is not possible to draw conclusions whether the models in this thesis overestimated the flood extent and flood depth or the Stockholm model underestimated since neither of the models are calibrated. Stockholm Stad stated that their model should only be used for a comprehensive picture and not grounds for planning as more detailed analyses are required (Stockholms stad 2023b). The models set up in this thesis also carries uncertainties caused by similar simplifications.

When examining the plotted results from overland flood there was a few observed deviations from the previously established pattern. As already mentioned, evaluation point 13 where clay 5^{th} generated the highest overland flow and sandy loam 95^{th} the third highest after clay median. Clay median also had two large peaks which can be seen in Figure 13. The two large peaks might be caused by overland flow from surrounding areas upstream but that would highly likely also cause clay 5^{th} and clay 95^{th} to have double peaks based on the pattern from the overland flow at the other evaluation points. The flood depth when simulating with clay median also caused the highest flood depth in this location. Because of this, one could assume there to be a discretisation error in this location and the results in evaluation point 13 are not representative. The discretisation error could possibly be solved by increasing the resolution or lowering the time step.

Another evaluation point that showed a deviation from the pattern was evaluation point 9, see Figure 13, where all sandy loam generated higher maximum surface runoff than all clay and sand causes almost as high overland flow as the other soils. Evaluation point 9 is located in a viaduct in Farsta-Larsboda and is an impervious surface and will therefore not directly generate overland flow due to saturated soil. The overland flow in this evaluation point is from precipitation and overland flow generated from upstream surrounding areas.

Evaluation point 7, 13, 15 and 16 showed double peaks in the graphs for overland flow and both 7 and 15 reached maximum overland flow for clay at 3 hours and 2 hours and 25 minutes respectively, see Figure 9, Figure 13, Figure 10 and Figure 11. This is due to overland flow from surrounding upstream areas reaching the evaluation points. The first peak occurs during/slightly after peak rain intensity. When the rain event starts to subside the direct overland flow from saturated soil decreases and when excess overland flow from upstream area reaches the evaluation point it increases again. The large delay in time to reach peak for evaluation point 7 and 15 is due to their locations, 30 m upstream the catchment outlets.

A few of the hydrographs showed a spikey and irregular response. This could be solved by lowering the time step, but this would also increase the run time for the simulation and since it did not drastically affect the results it was not necessary.

The maximum measured overland flow in Fagersjö catchment was 48.3×10^{-2} m^3/s in evaluation point 3 and 12.63×10^{-2} m^3/s in evaluation point 16 in Farsta-Larsboda catchment. The high value for evaluation point 3 is due to its location in a steep slope, accelerating surface transport causing high overland flow in that particular point. For some of the evaluation points (1, 7, 8 and 15, see Figure 9, Figure 18 and Figure 10) overland flow for some of the soils did not reach zero at the end of simulation. This indicates that the simulation time was too short. Evaluating the maximum overland flow and time to reach peak overland flow in the evaluation points this

was not an issue since they both occurred before end of simulation. However, this did cause complications when analysing discharge from at the catchment outlet.

The measured discharge at the cross-section at the outlet in Fagersjö catchment all reached zero at the end of the simulation, as seen in Figure 14, but this was not the case for discharge in Farsta-Larsboda, see Figure 15. Neither of the clay soils or sandy loam soils reached zero which indicates that the simulation time for was not long enough. Due to the time frame of this thesis, it was not possible to re-do all these simulations and process the new results. The results for time to reach peak discharge and maximum discharge was not affected by this error, but total cumulative discharge, especially for the clay soils, is expected to be higher than presented results in Table 10 . Despite this error, the established result pattern still stands.

An interesting observation from the discharge results was that the total cumulative discharge in Fagersjö catchment was higher than in Farsta-Larsboda catchment (74.3 m^3 and 46.7 m^3) even though percentage of impervious surfaces was higher in Farsta-Larsboda. One possible explanation for this is the size of Farsta-Larsboda catchment. The overland flow has to "travel" longer distances to reach the outlet of the catchment with pervious surfaces along the path where it is possible for the water to infiltrate since sand has high infiltration rate and did not stay saturated for long. This would also explain the delay in time to reach peak discharge in Farsta-Larsboda compared to Fagersjö catchment. Farsta had a very steep peak for discharge around the same time as peak rain intensity (55-60 minutes into simulation). This indicates that the discharge was overland flow from nearby upstream area. For all clay soils, Farsta-Larsboda had a small peak at 1:25 hrs and then reached maximum at 2:30 hrs into simulation. Similarly, to already discussed multiple peaks for overland flow, this is due to upstream overland flow reaching the catchment outlet.

One simplified way to estimate if the second peak in discharge for Farsta-Larsboda, see Figure 15, is somewhat representative in time is by doing an estimate calculation of time of concentration. Time of concentration is the time needed for runoff to travel from the most remote point in the catchment to the catchment outlet (Svenskt vatten 2019). It is calculated by finding the longest flow path in the catchment and divide it by an estimated speed of water through the catchment. For Farsta-Larsboda the longest flow path was approximately 2530 m and an estimate of 0.3 m/s in speed (Svenskt vatten 2019). This gives a time of concentration of 02:50, 20 min later than the second peak for all clay soils in Farsta-Larsboda. The second peak can therefore be assumed to be valid and to be caused by upstream overland flow.

4.2 MODEL AND VARIABLE UNCERTAINTIES

The major simplifications done in this thesis was the assumption that all green areas within the catchment are lawns and have the same soil type. This is not realistic in urban areas. Urban green areas may be grass covered, but also often have trees (or in Fagersjö catchment a whole forest) and bushes planted. The assumption of the homogenous soil type would only be applicable if the urban area only had one green area, and possibly not even in that scenario. The decision to not have a coupled model with a collection system may been seen as major since the recommendation for scenarios when it is acceptable to do this is when modelling with design storms with a return period of 100 years or higher (MSB 2013). Indicating that a 100-year return period is the breaking point for this simplification.

A very common simplification, also done in this thesis, was to only use two different Manning's number, one for pervious and one for impervious surfaces which was recommended by MSB (2014). The third one added for lake did not affect the results, it only slowed down the flow out of the model domain to avoid possible modelling errors. The surface roughness affects the flow resistance and therefore also overland flow, flood extent and flood depth (MSB 2017). By

adding more Manning's number (for example other vegetation types and roofs) the outcome might have been different.

When constructing both models, the initial aim was to use 1 by 1 m resolution for the grids. This gave computation time of 27 hours for Fagersjö area and over 48 hours for Farsta-Larsboda area which highly restricted the amount of simulation runs possible within the time frame. Instead, the resolution was resampled to 2 by 2 m for both model areas, which is still higher resolution then the minimum recommended resolution of 4 by 4 meters in urban areas but do cause uncertainties, especially for cells containing houses or roads that might be larger or smaller in the model than in reality (MSB 2017).

The decision to only have one input with sand, and not multiple with different antecedent conditions, was a quick solution to obtain data for this thesis since it was not possible to obtain any equations from the method Tyréns currently uses. For the same reason the infiltration rate was set to constant throughout the simulation. To have multiple antecedent conditions would not have affected the established pattern of the results due to sand soils having such high infiltration compared to sandy loam and clay, which also would apply to infiltration curves instead of a constant infiltration rate.

Usually, it is industry standard to use constant infiltration rates when conducting cloudburst modelling to obtain a comprehensive review of potential flood risks in an area[1] but infiltration is a non-linear time-dependent process (Schumann 1998). Using a constant value does not depict the infiltration accurately. The infiltration curves provided by Tyréns was determined a more accurate way to represent infiltration during a rainfall, however, since there was no infiltration data after the rain series ended, the infiltration rate after the rain event was assumed to be constant. In cases where overland flow occurs, the infiltration rate actually gradually decreases after a rain event (Schumann 1998). This indicates that the provided infiltration curves do represent infiltration more accurate than a constant value during the rain event but neither of them are accurate after the rain event. The depth of the soil profile used to obtain the infiltration curves was 2.5 m. When investigating actual soil depth in Fagersjö and Farsta-Larsboda (due to simplifications, both model areas was determined synthetic), variations between 0-20 m was found in both catchments with a majority of 0-3 m (SGU 2023). Using a 2.5 m soil profile is therefore justified.

As previously mentioned, there are many methods to generate rainfall for simulations. In this thesis CDS was chosen, which is also the most used. One important input parameter to generate the CDS is the skewness factor, the r-value, which determines when in time peak rainfall intensity is reached. In this thesis 0.37 was chosen on recommendations for Swedish conditions (Svenskt vatten 2011; Berggren et al. 2014) but choosing a different r-value would have affected the results. Alhstedt (2022) found that with increasing r-value overland flow and discharge increased and time to reach peak discharge was delayed. When comparing infiltrated rain using a r-value of 0.1 or 0.8, a smaller proportion of design storm peak was infiltrated with 0.8 compared to 0.1. Alstedt concluded that this was due to the soil already being saturated before peak rainfall intensity was reached with 0.8 (Ahlstedt 2022). The CDS was also based on general Swedish conditions. To obtain more accuracy, the CDS could be generated from historical rain data sourced more locally to the model areas.

The choice of location of evaluation points can be deemed biased. To ensure all evaluation points produced results for at least one evaluation variable they had to be picked based on certain criteria. This also caused the points to not be spatially distributed throughout the model domain. To avoid bias and ensure spatial distribution, a much larger selection would have been

[1] Johan Kjellin, Vattenspecialist at Tyréns AB

necessary to gain results were conclusions could be drawn from since many cells in the model areas did not generate runoff or was not flooded.

The factor causing largest uncertainty in the results is that the models are not calibrated. This is also common for "real life" modelling flood predictions since it rarely exists observations of for example flood depth or flood extent (MSB 2017). Since the model areas are assumed to be synthetic due to the simplifications, this is not as important as if the thesis would have been a case study of a real storm event. Same conclusions can be drawn from the decision to not use historical rain observations from the actual areas but using one for general conditions in Sweden.

4.3 FUTURE STUDIES

The findings from this study shows that the textural distribution of soils in urban green areas have a large impact on both flood extent and overland flow. As did antecedent soil moisture content but not to the same extent. Due to the time frame of this thesis only three different soils conditions could be examined. To include a larger variety of soil types would be interesting, preferable to conduct a field study to determine soil types in Swedish urban green areas since this could not be found during the literature study. By doing this, it could possibly determine if the recommended soil type by AMA is the best option for urban green areas in Sweden. When investigating percentage of flooded model area, it would also have been interesting to add a duration perspective, as in how long cells were flooded (flood depth larger than 0.15 m) during the simulations. This was somewhat done by looking at generated runoff in the evaluation points, as long as runoff was generated the flood depth in that specific location was larger than 0 m. But, by looking at all durations for all flooded cells one might be able to detect larger differences of flood duration between model areas with high percentage of impervious areas compared to areas with low percentages which may also affect the consequences of a flood.

There were many simplifications of reality that had to be done to conduct this study, one being that all urban green areas within the model area were assumed to be lawns with same soil type. In the actual Fagersjö and Farsta-Larsboda catchment there was a variety of lawn, trees, and bushes. In further studies it would be more realistic to have different types of green areas, alternating the vegetation which also requires multiple coefficients for surface roughness. As mentioned earlier in this thesis, the soil in urban green areas gets compacted which can affect the infiltration. To conduct a field study and obtain experimental soil data from the green areas would therefore be interesting to be able to compare that with infiltration data obtained from Hydrus 1D simulations based solely on soil texture distribution.

There are many different methods to generate and simulate a storm event in a surface runoff model. In this thesis, a two hours CDS with a return period of 100 years based on general Swedish conditions was used. It would be interesting to include either different durations or return periods to see how it effects the flood extent and generated runoff and to use local precipitation data to generate the CDS instead of general Swedish conditions. It would also be interesting to include different climate factors for the precipitation event that accounts for climate change. This could help understand the importance of using urban green areas as a mitigation tool for climate change.

As previously mentioned, to determine the accuracy of a constructed model it is important to calibrate it. Due to lack of observations of flood extent or flood depth this is in general not possible. To improve the models used in this thesis one could create a coupled model which includes the collection system or use a reduction factor on the precipitation to account for it. This would especially be interesting since multiple sources stated that if a precipitation event with a return period of 100 years or more was used, it was not necessary to include a collection

system. This was because of the amount of rain the collection system can manage is so small compared to the total amount of precipitation so it can be seen as negligible.

5 CONCLUSIONS

The objective of the thesis was to examine the hydraulic response when varying soil characteristics affecting infiltration. The same result pattern could be determined for all evaluation variables: with increasing infiltration and decreasing soil moisture content the flood extent, flood depth, overland flow and discharge decreased. With the usage of sand in all urban green areas the hydraulic response was the smallest and with clay 95th it was the largest.

Fagersjö was more sensitive to changes in both soil type and antecedent soil moisture when analysing flood extent compared to Farsta-Larsboda. This was because of a higher percentage of pervious area in the Fagersjö catchment compared to Farsta-Larsboda. Changes in soil moisture content affected the results from sandy loam the most. The largest flood extent measured in Fagersjö was 13.8 % and 13.5 % in Farsta-Larsboda with clay 95th. Sand caused least flood extent, 4.19 % in Fagersjö and 7.13% in Farsta-Larsboda.

When analysing maximum flood depth in chosen evaluation points the largest difference was 1.80 m between sand and mean maximum flood depth with clay in evaluation point 2. The largest difference in antecedent moisture content was also at evaluation point 2, being 0.14 m between sandy loam 5th and 95th.

The highest measured overland flow in Fagersjö catchment for an evaluation point was 48.3×10^{-2} m^3/s with clay 95th, the lowest in that same location was 19.3×10^{-2} m^3/s with sand. In Farsta-Larsboda, the highest measured overland flow was 12.63×10^{-2} m^3/s with clay 95th and the lowest in that same evaluation point was 5.85×10^{-2} m^3/s, also with sand. Time to reach peak overland flow varied between 45 minutes and 3 hours for the different soil types. The large time delay was caused by the location of the evaluation points, being close to the catchment outlets. The largest time difference between antecedent soil moisture was 10 minutes.

The highest measured maximum discharge in both catchments were with clay 95th, 1.39 m^3/s in Farsta-Larsboda and 2.44×10-1 m^3/s in Fagersjö. The lowest maximum in both catchments were achieved with sand, 4.28×10-2 m^3/s in Farsta-Larsboda and 5.54×10^{-2} m^3/s in Fagersjö. In Fagersjö, a deviation from the result pattern was found with clay 5th. It was generating 1×10^{-3} m^3/s higher maximum discharge than clay median but clay median generated larger total cumulative discharge so this deviation can be assumed negligible when concluding the result pattern. Time to reach peak discharge only varied 5 minutes between the different soil types and zero minutes between antecedent soil moisture in Fagersjö catchment. In Farsta-Larsboda the difference between antecedent soil moisture was still zero but varied with 55 minutes (sand), 1 hr 25 min (sandy loam) and 2 hrs 30 min (clay) to reach peak discharge. The delay in time to peak for sandy loam and clay was determined to be caused by the size of the catchment. The results for total cumulative discharge are underestimated in Farsta-Larsboda catchment for all simulations with clay and sandy loam. This was due to simulation time being too short. Conclusions for same determined result pattern could still be drawn but the total cumulative discharge for these simulations would be higher.

It is possible that the recommended soil type by AMA is not the best recommendation if the aim of an urban green area is to mitigate floods. It would need further testing but by increasing the percentage of sand it might be possible to improve the infiltration rates in Swedish urban green areas and further prevent flooding.

Differences in antecedent soil moisture content was found to have a larger impact in Fagersjö catchment than in Farsta-Larsboda catchment and caused largest difference in hydraulic

response for the soil type sandy loam. But, in comparison to the difference in results between soil type and between antecedent moisture content, antecedent soil moisture content was not deemed critical in floods.

6 REFERENCES

Ahlmer, A.-K., Cavalli, M., Hansson, K., Koutsouris, A.J., Crema, S. & Kalantari, Z. (2018). Soil moisture remote-sensing applications for identification of flood-prone areas along transport infrastructure. *Environmental Earth Sciences*, 77 (14), 533. https://doi.org/10.1007/s12665-018-7704-z

Ahlstedt, O. (2022). *How variations of the duration and time to peak of the Chicago Design Storm affect the hydraulic response, as well as the areas contributing to peak runoff, of a synthetic urban catchment area*. Uppsala university.

Berggren, K., Packman, J., Ashley, R. & Viklander, M. (2014). Climate changed rainfalls for urban drainage capacity assessment. *Urban Water Journal*, 11 (7), 543–556. https://doi.org/10.1080/1573062X.2013.851709

Boverket (2022). *Grönplanera för anpassning till ett ändrat klimat*. *Boverket*. https://www.boverket.se/sv/PBL-kunskapsbanken/teman/gronplan/darfor-behovs/andrat_klimat/ [2023-03-30]

Broekhuizen, I., Muthanna, T.M., Leonhardt, G. & Viklander, M. (2019). Urban drainage models for green areas: Structural differences and their effects on simulated runoff. *Journal of Hydrology X*, 5, 100044. https://doi.org/10.1016/j.hydroa.2019.100044

Cea, L. & Costabile, P. (2022). Flood Risk in Urban Areas: Modelling, Management and Adaptation to Climate Change. A Review. *Hydrology*, 9 (3), 50. https://doi.org/10.3390/hydrology9030050

Crawford, S.E., Brinkmann, M., Ouellet, J.D., Lehmkuhl, F., Reicherter, K., Schwarzbauer, J., Bellanova, P., Letmathe, P., Blank, L.M., Weber, R., Brack, W., Van Dongen, J.T., Menzel, L., Hecker, M., Schüttrumpf, H. & Hollert, H. (2022). Remobilization of pollutants during extreme flood events poses severe risks to human and environmental health. *Journal of Hazardous Materials*, 421, 126691. https://doi.org/10.1016/j.jhazmat.2021.126691

DHI (2023a). MIKE+ - User Guide - 2D Overland. DHI. https://manuals.mikepoweredbydhi.help/latest/MIKEPlus.htm

DHI (2023b). *MIKE+ - User guide - Model Manager*. https://manuals.mikepoweredbydhi.help/latest/MIKEPlus.htm [2023-04-17]

DHI (2023c). *MIKE 21 Flow Model FM - Hydraulic Module - User Guide*. https://manuals.mikepoweredbydhi.help/2017/MIKE_21.htm [2023-04-17]

Duan, R., Fedler, C.B. & Borrelli, J. (2011). Field evaluation of infiltration models in lawn soils. *Irrigation Science*, 29 (5), 379–389. https://doi.org/10.1007/s00271-010-0248-y

Ebrahimian, A., Sample-Lord, K., Wadzuk, B. & Traver, R. (2020). Temporal and spatial variation of infiltration in urban green infrastructure. *Hydrological Processes*, 34 (4), 1016–1034. https://doi.org/10.1002/hyp.13641

Environment Agency (2019). *What is the Risk of Flooding from Surface Water Map?* Bristol: Environment Agency.

Fidal, J. & Kjeldsen, T.R. (2020). Accounting for soil moisture in rainfall-runoff modelling of urban areas. *Journal of Hydrology*, 589, 125122. https://doi.org/10.1016/j.jhydrol.2020.125122

Gävle Kommun (2022). *Så drabbades Gävle av skyfallet 2021*. *Gävle kommun*. https://www.gavle.se/kommunens-service/sa-drabbades-gavle-av-skyfallet-2021/ [2023-03-30]

Gong, Y., Liang, X., Li, X., Li, J., Fang, X. & Song, R. (2016). Influence of Rainfall Characteristics on Total Suspended Solids in Urban Runoff: A Case Study in Beijing, China. *Water*, 8 (7), 278. https://doi.org/10.3390/w8070278

Grahn, P. & Stoltz, J. (2022). *Indikatorer för hälsopromoverande urbana grönområden*. (7043). Stockholm: Naturvårdsverket.

Haghnazari, F., Shahgholi, H. & Feizi, M. (2015). Factors affecting the infiltration of agricultural soils: review. *International Journal of Agronomy and Agricultural Research (IJAAR)*, (6), 21–35

Hallberg, L. (2021). *Stora översvämningar i Gävle*. *Transportarbetaren*. https://www.transportarbetaren.se/stora-oversvamningar-i-gavle/ [2023-06-02]

Hendriks, M.R. (2010). *Introduction to physical hydrology*. Oxford ; New York: Oxford University Press.

Kuebler, M. (2022). How climate change is shifting the water cycle. *Deutche Welle*,. https://www.dw.com/en/water-cycle-climate-change-sponge-cities-drought-flooding-monsoon-hindu-kush-himalayas/a-63332091 [2023-03-30]

Lan, T., Guo, S.-W., Han, J.-W., Yang, Y.-L., Zhang, K., Zhang, Q., Yang, W. & Li, P.-F. (2019). Evaluation of physical properties of typical urban green space soils in Binhai Area, Tianjin, China. *Urban Forestry & Urban Greening*, 44, 126430. https://doi.org/10.1016/j.ufug.2019.126430

Markolf, S.A., Chester, M.V., Helmrich, A.M. & Shannon, K. (2021). Re-imagining design storm criteria for the challenges of the 21st century. *Cities*, 109, 102981. https://doi.org/10.1016/j.cities.2020.102981

MSB (2013). *Pluviala översvämningar - Konsekvenser vid skyfall över tätorter, en kunskapsöversikt*. (MSB567-13). Göterborg & Lund.

MSB (2014). *Kartläggning av skyfalls påverkan på samhällsviktig verksamhet - Framtagande av metodik för utredning på kommunal nivå*. (MSB694-maj 2014). Malmö.

MSB (2016). *Nederbörd och översvämningar i framtidens Sverige*. (978-91-7383-641–8). Göteborg.

MSB (2017). *Vägledning för skyfallskartering - Tips för genomförande och exempel på användning*. (MSB1121-augusti 2017)

MSB & SGI (2021). *Riskområden för ras, skred, erosion och översvämning, Redovisning av regeringsuppdrag enligt regeringsbeslut M2019/0124/Kl*. Linköping: Statens geotekniska institut.

Naturvårdsverket (2023). *Effekter i Sverige*. [Myndighet]. https://www.naturvardsverket.se/amnesomraden/klimatforandringar/klimatet-i-framtiden/effekter-i-sverige/ [2023-03-30]

NE (2023). Ytavrinning. https://www-ne-se.ezproxy.its.uu.se/uppslagsverk/encyklopedi/l%C3%A5ng/ytavrinning [2023-03-30]

Olsson, J., Berg, P., Eronn, A., Simonsson, L., Södling, J., Wern, L. & Yang, W. (2017). Extremregn i nuvarande och framtida klimat - Analyser av observationer och framtidsscenarier. (47)

Prammefors, A. & Wass, A.-M. (2018). Forskaren: Parker hade förhindrat översvämningen vid resecentrum. *Sveriges Radio*. https://sverigesradio.se/artikel/7012595 [2023-06-02]

Ren, X., Hong, N., Li, L., Kang, J. & Li, J. (2020). Effect of infiltration rate changes in urban soils on stormwater runoff process. *Geoderma*, 363, 114158. https://doi.org/10.1016/j.geoderma.2019.114158

Saleh, F. (2021). *Modeling the Perfect Storm: How Antecedent Conditions Can Compound the Severity of Flood Tail Risk Events*. https://www.rms.com/blog/2021/09/29/modeling-the-perfect-storm-how-antecedent-conditions-can-compound-the-severity-of-flood-tail-risk-events [2023-05-08]

Scalgo Live (2023). *SCALGO Live Documentation - Country Specific - Sweden - SCALGO*. https://scalgo.com/en-US/scalgo-live-documentation/country-specific/sweden [2023-04-13]

Schumann, A.H. (1998). Infiltration: Introduction. In: Herschy, R.W. & Fairbridge, R.W. (eds) *Encyclopedia of Hydrology and Water Resources*. Dordrecht: Springer Netherlands. 418–418. https://doi.org/10.1007/978-1-4020-4497-7_129

SGU (2023). *Kartvisaren Jorddjup*. https://www.sgu.se/produkter-och-tjanster/kartor/kartvisaren/jordkartvisare/jorddjup/ [2023-06-09]

SMHI (2022a). *2021 - Skyfall i Gävle*. https://www.smhi.se/kunskapsbanken/hydrologi/historiska-oversvamningar/2021-skyfall-i-gavle-1.175548 [2023-03-30]

SMHI (2022b). *Klimatindikator - nederbörd*. https://www.smhi.se/klimat/klimatet-da-och-nu/klimatindikatorer/klimatindikator-nederbord-1.2887 [2023-03-30]

SMHI (2023a). *Ladda ner meteorologiska observationer*. https://www.smhi.se/data/meteorologi/ladda-ner-meteorologiska-observationer#param=precipitationHourlySum,stations=all,stationid=97510 [2023-03-30]

SMHI (2023b). *Olika typer av översvämningar*. https://www.smhi.se/kunskapsbanken/hydrologi/oversvamningar/olika-typer-av-oversvamningar-1.176299 [2023-03-30]

Stockholms stad (2023a). *Miljödataportalen - Stockholms stad*. https://miljodataportalen.stockholm.se/ [2023-06-12]

Stockholms stad (2023b). *Stockholms skyfallsmodell - Stockholms miljöbarometer*. https://miljobarometern.stockholm.se/klimat/klimatanpassning/skyfall/stockholms-skyfallsmodellering/ [2023-06-20]

Svensk Byggtjänst (2020). *AMA Anläggning 20*. Svensk Byggtjänst.

Svenskt vatten (2011). *Nederbördsdata vid dimensionering och analys av avloppssystem*. 1. utgåvan. Stockholm: Svenskt vatten. (Publikation / Svenskt vatten, 104)

Svenskt vatten (2019). *Avledning av dag-, drän- och spillvatten. Funktionskrav, hydraulisk dimensionering och utformning av allmänna avloppssystem*. 1. utgåvan. Stockholm: Svenskt vatten. (Publikation / Svenskt vatten, 110)

SVT Nyheter (2018). Stora översvämningar över hela Uppsala. *SVT Nyheter*. Uppsala. https://www.svt.se/nyheter/lokalt/uppsala/oversvammning-vid-strandbogatan-i-uppsala [2023-03-30]

Swedish Commission on Climate and Vulnerability (ed.) (2007). *Sweden facing climate change: threats and opportunities ; final report from the Swedish Commission on Climate and Vulnerability*. Stockholm: Fritze. (Statens offentliga utredningar; 2007,60)

Thurin, S., Toren, F. & Samuelsson, H. (2018). *Skyfallsmodellering Stockholm stad*

USDA (2020). *HYDRUS-1D Model*. https://www.ars.usda.gov/pacific-west-area/riverside-ca/agricultural-water-efficiency-and-salinity-research-unit/docs/model/hydrus-1d-model/ [2023-05-08]

USGS (2023). *Surface Runoff and the Water Cycle | U.S. Geological Survey*. https://www.usgs.gov/special-topics/water-science-school/science/surface-runoff-and-water-cycle [2023-05-05]

Yolcubal, I., Brusseau, M.L., Artiola, J.F., Wierenga, P. & Wilson, L.G. (2004). Environmental physical properties and processes. In: *Environmental Monitoring and Characterization*. Elsevier. 207–239. https://doi.org/10.1016/B978-012064477-3/50014-X

APPENDICES

APPENDIX A

Soil characteristics influencing infiltration in green areas

Soil texture

Soil types are usually categorised based on content of sand, silt, and clay. These categories are based on the particle size where sand has the largest particles and clay the smallest. Soil texture is an instrument to determine the class of a soil based on their physical texture. A qualitative way to determine soil texture is by "feel" if it is fine and smooth or coarse. Quantitively, soil texture is determined by measuring the distribution of particle sizes. There are several particle size classifications but the most widely used is developed by USDA (the U.S. Department of Agriculture) which also includes gravel as a main category of soil (Yolcubal et al. 2004). The USDA particle size classification is shown in Table 8 below and Figure 16 shows the USDA soil texture triangle graphically.

Table 8. Adapted table of USDA Classification of soil particle size (Yolcubal et al. 2004)

Type	Diameter (mm)
sand	0.05-2
silt	0.002-0.05
clay	< 0.002

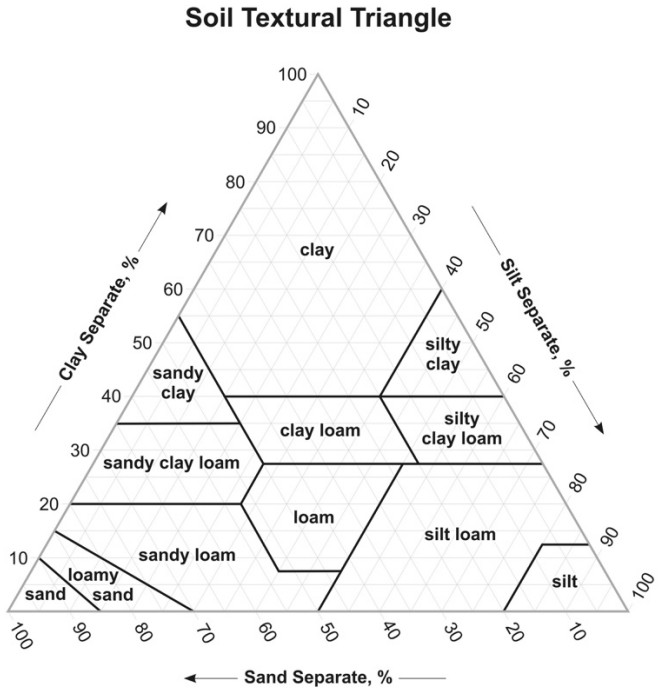

Figure 16. USDA soil texture triangle.

Porosity

The porosity of a soil describes the ratio of void space to bulk volume (fraction of "empty" space in soil) and is largely dependent on the grain-size distribution of the soil and the grain's packing arrangement (Yolcubal et al. 2004).

Soil moisture

Soil moisture, also called volumetric water content, for a soil is defined as the volume fraction or volume percentage of water filled pores in a soil. Soil moisture influence the drainage mechanism in a soil. Dry soil (soil with a low volumetric moisture content) has, very simply put, a large suction (strongly negative matric potential). When water is added to a dry soil the water will first be sucked into the smaller pores in the soil. When these pores are filled, the larger pores will begin to fill. This is because smaller pores have larger suction power than larger ones. In reverse/vice versa, when a wet soil (soil with high volumetric moisture content) is drained the larger pores will drain first. If a soil is saturated (all pores are filled with water) the volumetric water content equals the porosity of the soil (Hendriks 2010). And if there is a continued inflow of water into a fully saturated soil, surface runoff will be generated.

The influence of soil compaction on infiltration

Multiple studies have shown that compaction of soil in urban green areas has a negative impact on infiltration rates. When compaction of soil occurs the amount of macropores, and pore space is reduced (bulk density increase) which decreases both infiltration and drainage of the soil. This leads to a slower infiltration of stormwater runoff (Ebrahimian et al. 2020). One study stated that infiltration rate for a soil when compacted was reduced with 70-99 % and pervious covers when compacted potentially behaves as impervious. Compaction of soil in urban green areas can come from human activities such as parking vehicles, foot traffic and playing sports etc. or over time due to physical and chemical processes in the soil. Soil disturbance is another reason for soil compaction and in urban green areas soil disturbance is often caused by construction or site activities (Ebrahimian et al. 2020).

APPENDIX B

Table 9. Chosen soil types with corresponding content and source

Soil type	ID*	Depth (m)	Sand (%)	Silt (%)	Clay (%)	Sample location	Source
Sandy loam	A	N/A	60	25	15	N/A	(Svensk Byggtjänst 2020)
Clay	“PFS”	0–30	20.96	8.54	63.68	Binhai Area, Tianjin, China	(Lan et al. 2019)
Sand	“PSS2”	0–10	93.66	4.29	2.05	Texas, USA	(Duan et al. 2011)

*ID is given ID for soil sample in article

APPENDIX C

Infiltration curves

During this thesis, a parallel project at Tyréns was conducted with the aim to find more detailed ways to represent the infiltration and antecedent moisture in soils in MIKE+. The built in infiltration modules have very simplified ways to describe infiltration and antecedent conditions (often assumed to be constant) which may lead to over- or underestimating surface runoff. This project was conducted in Hydrus 1D, a modelling environment that can be used for simulation movement of water in variably saturated media (USDA 2020).

Firstly, a historical rain series of 15 years was simulated for all soil types with a soil profile of 2.5 m, with ground water level at the bottom of the profile. All rain event that met the requirements of the definitions of a rain event were selected from these simulations with the definition being 3-hour antecedent dry weather period, total depth of at least 2 mm and an average intensity of at least 0.01 mm/h (Broekhuizen et al. 2019). This resulted in approximately 280 rain events for each soil used in this thesis. At the start of each rain event, the soil profiles antecedent soil moisture content were extracted in the form of a pressure profile. From these datasets of pressure profiles, the 5^{th}, 50^{th} and 95^{th} percentile was chosen for each soil type, 5^{th} being the low antecedent soil moisture content and 95^{th} high antecedent soil moisture content in the data sets.

The three percentiles for each soil type were then used as initial soil profiles in Hydrus 1D. The rain data used for these simulations was five different empirical hyetographs of 2 hours precipitation extremes produced by SMHI from observations in the middle region of Sweden (Olsson et al. 2017). All five hyetographs had a return period of 100 years. The results from these simulations was then interpolated and curve fitted to obtain an infiltration curve for infiltration rate over accumulated rain depth for each soil type and corresponding antecedent soil moisture content (given as a percentile). An example of an infiltration curve can be seen in Figure 5 in section 2.3.4. The blue circles are the results from simulations with the five different hyetographs and the red curve is the infiltration curve derived from interpolation.[2]

[2] Sara Ekeroth, Utredare Vatten at Tyréns AB

APPENDIX D

Overland flow at evaluation points

Plots of overland flow at evaluation points not included in Results in section 3.3.

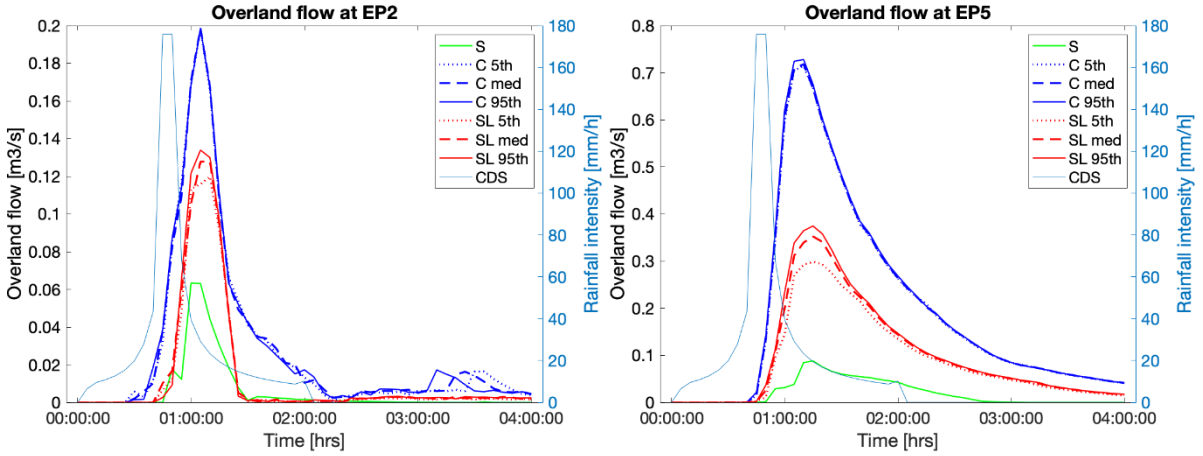

Figure 17. Overland flow at evaluation point 2 (left) and 5 (right). Different colours indicate different soil type and marker type different antecedent soil moisture. On the first y-axis, discharge at the cross-section upstream outlet is displayed, on the second y-axis the rain intensity for the CDS is displayed.

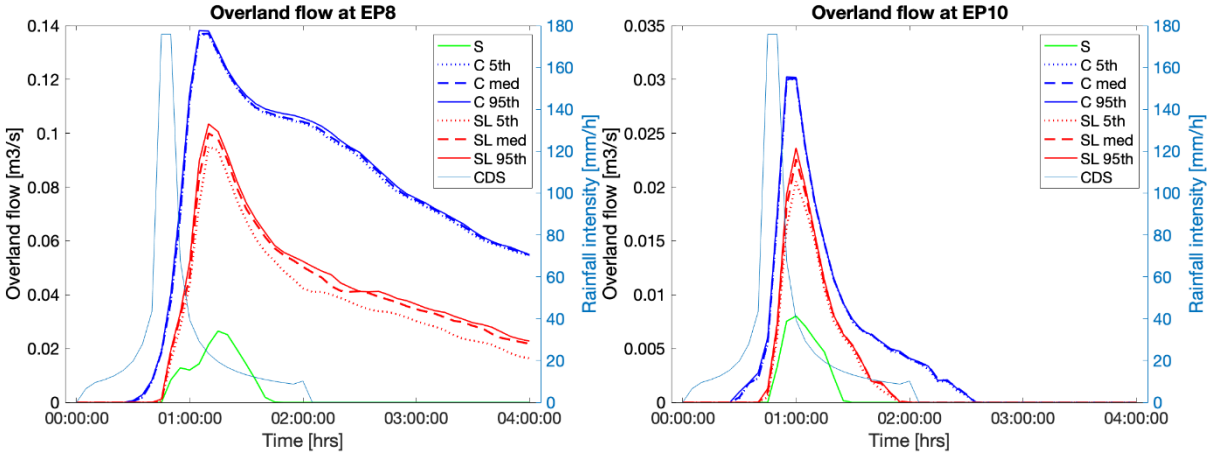

Figure 18. Overland flow at evaluation point 8 (left) and 10 (right). Different colours indicate different soil type and marker type different antecedent soil moisture. On the first y-axis, discharge at the cross-section upstream outlet is displayed, on the second y-axis the rain intensity for the CDS is displayed.

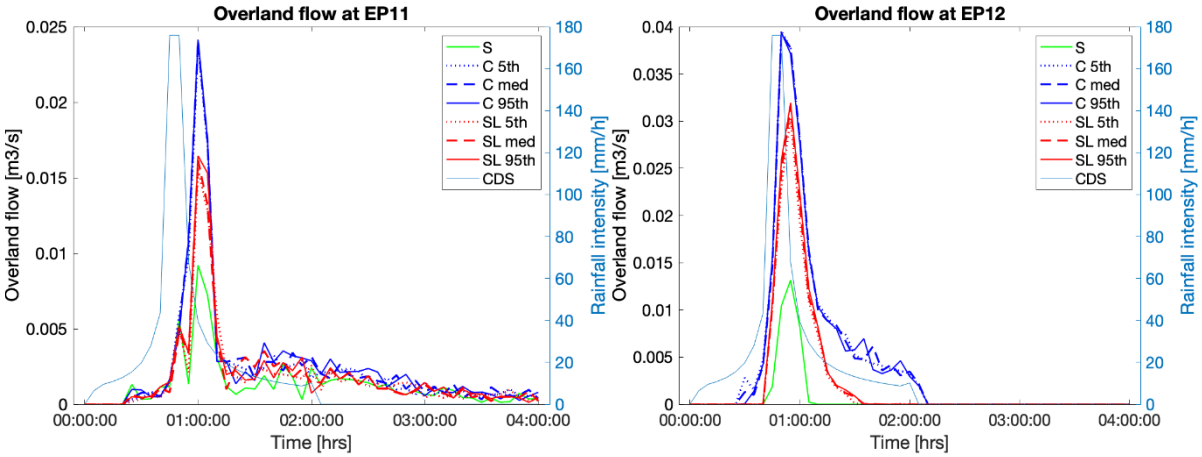

Figure 19. Overland flow at evaluation point 11 (left) and 12 (right). Different colours indicate different soil type and marker type different antecedent soil moisture. On the first y-axis, discharge at the cross-section upstream outlet is displayed, on the second y-axis the rain intensity for the CDS is displayed.

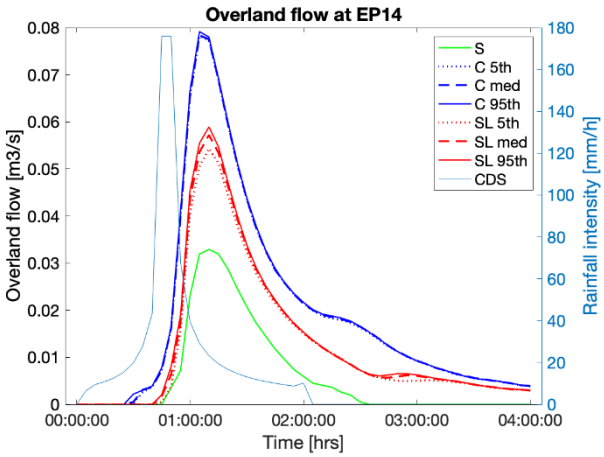

Figure 20. Overland flow at evaluation point 14. Different colours indicate different soil type and marker type different antecedent soil moisture. On the first y-axis, discharge at the cross-section upstream outlet is displayed, on the second y-axis the rain intensity for the CDS is displayed.

Table 10. Overland flow at evaluation points. T is "Time to peak" in hrs:min and R is maximum runoff on 10^{-2} m^3/s.

		Sand	Clay 5th	Clay median	Clay 95th	Sandy loam 5th	Sandy loam median	Sandy loam 95th
EP1	T	00:45	01:20	01:20	01:20	01:55	01:45	01:45
	R	0.191	7.39	7.38	7.24	1.47	1.94	2.25
EP2	T	01:00	01:05	01:05	01:05	01:10	01:10	01:05
	R	6.33	19.8	19.7	19.9	12.0	12.8	13.4

EP3	T	01:00	01:00	01:00	01:00	01:00	01:00	01:00
	R	19.3	47.8	48.0	48.3	38.0	39.4	40.1
EP4	T	0	0	0	0	0	0	0
	R	0	0	0	0	0	0	0
EP5	T	01:15	01:10	01:10	01:10	01:15	01:15	01:15
	R	8.80	71.4	71.8	72.8	29.8	35.2	37.5
EP6	T	01:00	01:00	01:00	01:00	01:00	01:00	01:00
	R	14.3	43.9	44.0	44.1	33.8	35.6	36.5
EP7	T	00:50	03:00	03:00	03:00	01:10	01:10	01:10
	R	0.188	4.14	4.19	4.29	1.17	1.33	1.40
EP8	T	01:15	01:10	01:10	01:10	01:10	01:10	01:10
	R	2.65	13.68	13.71	13.82	9.50	9.99	10.35
EP9	T	00:50	00:50	00:50	00:50	00:50	00:50	00:50
	R	17.0	20.4	20.1	19.2	25.2	26.4	26.8
EP10	T	01:00	01:00	01:00	01:00	01:00	01:00	01:00
	R	0.80	3.01	3.01	3.02	2.05	2.26	2.36
EP11	T	01:00	01:00	01:00	01:00	01:00	01:00	01:00
	R	0.921	2.37	2.40	2.42	1.55	1.62	1.64
EP12	T	00:55	00:50	00:50	00:50	00:55	00:55	00:55
	R	1.31	3.96	3.92	3.94	3.03	3.16	3.19
EP13	T	00:55	00:55	00:55	00:50	00:50	00:50	00:50
	R	0.007	0.218	0.192	0.144	0.048	0.030	0.185
EP14	T	01:10	01:05	01:05	01:05	01:10	01:10	01:10
	R	3.29	7.82	7.84	7.91	5.43	5.72	5.89
EP 15	T	01:05	02:25	02:20	02:20	01:05	01:05	01:00
	R	0.57	3.39	3.42	3.50	1.25	1.50	1.56

EP 16	T	01:25	01:10	01:10	01:10	01:15	01:15	01:15
	R	5.85	12.53	12.56	12.63	9.15	9.52	9.77

APPENDIX E

Comparison of maximum flood depth in MIKE+ versus Stockholm municipality's cloudburst model.

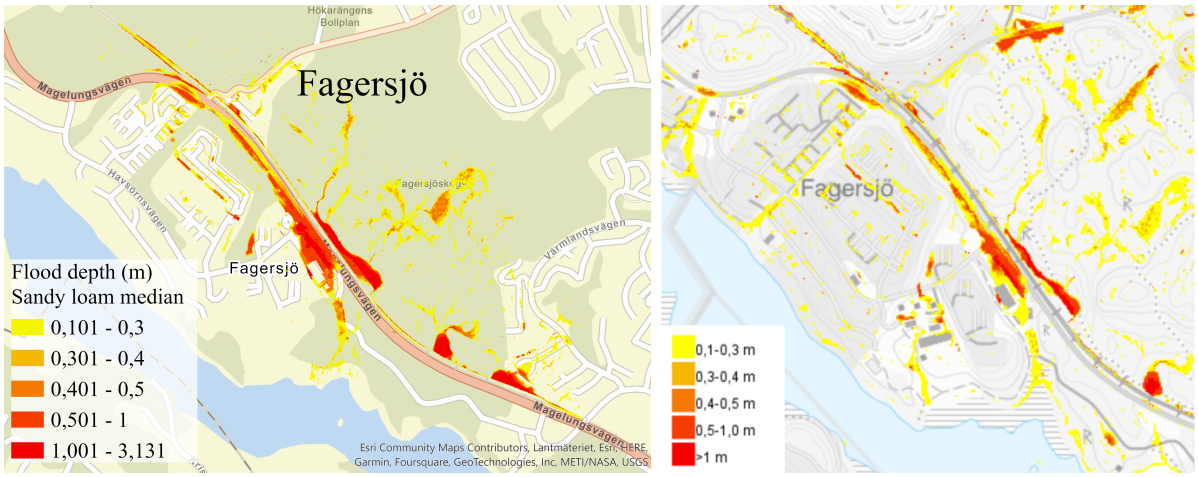

Figure 21. Maximum flood depth for sandy loam median in Fagersjö catchment. Modelled in MIKE+ to the left and Stockholm municipality's cloudburst model to the right (source: https://openstreetgs.stockholm.se/geoservice/api/ba9e5991-379f-4eb4-b6a3-e288a3730b2a/skyfall/wms or https://miljodataportalen.stockholm.se/).

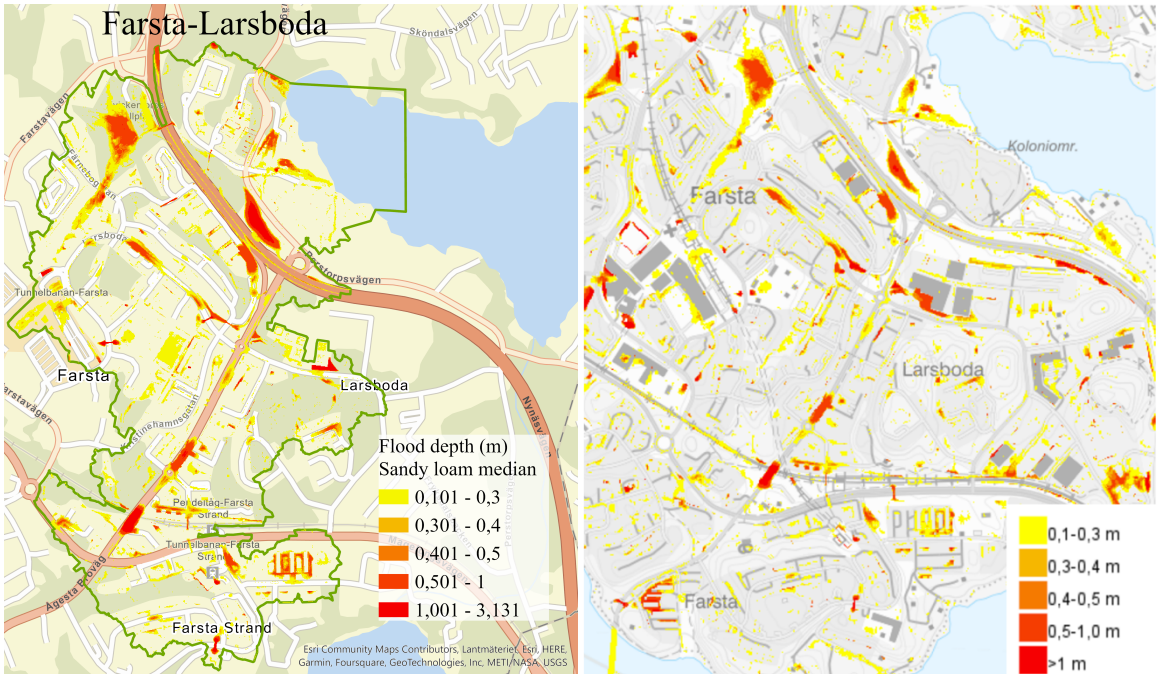

Figure 22. Maximum flood depth for sandy loam median in Farsta-Larsboda catchment. Modelled in MIKE+ to the left and Stockholm municipality's cloudburst model to the right (source: https://openstreetgs.stockholm.se/geoservice/api/ba9e5991-379f-4eb4-b6a3-e288a3730b2a/skyfall/wms or https://miljodataportalen.stockholm.se/).